Review article

Johannes Flick*, Nicholas Rivera and Prineha Narang*

Strong light-matter coupling in quantum chemistry and quantum photonics

https://doi.org/10.1515/nanoph-2018-0067
Received June 5, 2018; revised July 21, 2018; accepted August 7, 2018

Abstract: In this article, we review strong light-matter coupling at the interface of materials science, quantum chemistry, and quantum photonics. The control of light and heat at thermodynamic limits enables exciting new opportunities for the rapidly converging fields of polaritonic chemistry and quantum optics at the atomic scale from a theoretical and computational perspective. Our review follows remarkable experimental demonstrations that now routinely achieve the strong coupling limit of light and matter. In polaritonic chemistry, many molecules couple collectively to a single-photon mode, whereas, in the field of nanoplasmonics, strong coupling can be achieved at the single-molecule limit. Theoretical approaches to address these experiments, however, are more recent and come from a spectrum of fields merging new developments in quantum chemistry and quantum electrodynamics alike. We review these latest developments and highlight the common features between these two different limits, maintaining a focus on the theoretical tools used to analyze these two classes of systems. Finally, we present a new perspective on the need for and steps toward merging, formally and computationally, two of the most prominent and Nobel Prize-winning theories in physics and chemistry: quantum electrodynamics and electronic structure (density functional) theory. We present a case for how a fully quantum description of light and matter that treats electrons, photons, and phonons on the same quantized footing will unravel new quantum effects in cavity-controlled chemical dynamics, optomechanics, nanophotonics, and the many other fields that use electrons, photons, and phonons.

Keywords: first principles theory; quantum electrodynamical DFT; quantum optics; polaritonic chemistry; strong light-matter coupling.

***Corresponding authors: Johannes Flick and Prineha Narang,** John A. Paulson School of Engineering and Applied Sciences, Harvard University, 29 Oxford St, Cambridge, MA 02138, USA, e-mail: flick@seas.harvard.edu (J. Flick); prineha@seas.harvard.edu (P. Narang). https://orcid.org/0000-0003-0273-7797 (J. Flick); http://orcid.org/0000-0003-3956-4594 (P. Narang)
Nicholas Rivera: John A. Paulson School of Engineering and Applied Sciences, Harvard University, Cambridge, MA, USA; and Department of Physics, Massachusetts Institute of Technology, Cambridge, MA, USA

1 Introduction

From the strong coupling of a plasmonic mode with a few molecules to the collective strong coupling of many molecules to a single-cavity mode, impressive experimental demonstrations in the last decade have explored new regimes of light-matter coupling. Traditionally, the quantum nature of light has been the focus of the established field of quantum optics [1]; in recent years, however, other research disciplines, particularly the fields of excitonic and 2D materials science [2, 3] and quantum chemistry [4], have started to utilize the quantum nature of light. As a consequence, research in these fields has surged, driving the effective strength of the light-matter interaction to previously unobserved strong coupling regimes and thereby opening new avenues for using these effects for applications in quantum photonic, electronic, quantum information and energy technologies.

Driven by the ever-increasing capabilities in the fabrication of nanostructured systems, novel states of matter with hybrid light-matter character have been created that have not been observed before. In this regime, where light and matter meet on the same quantized footing, quasi-particles that have both light and matter character – "polaritons" – are formed.

Using the hybrid light-matter character of these polaritonic states, various experiments already have demonstrated that material properties can be modified and in some cases even improved in the regime of strong light-matter coupling.

One intriguing example is the new field of polaritonic chemistry [5], where chemical systems are studied under strong light-matter coupling. In this field, experimentalists have made tremendous progress recently; they have

coupled molecular resonators with a microcavity mode [6], demonstrating a host of effects such as altered chemical reactions [7, 8], altered field-effect mobility [9], altered Raman spectra [10], long-range strong coupling [11–13], and the selective manipulation of excited states [14], all of which have been achieved by a collective coupling of many emitters to the light field. In a different limit, the strong coupling of few molecules of chemical interest has been achieved in the field of nanoplasmonics, i.e. the plasmon-induced chemical reactions of a single molecule [15], and single-molecule redox chemistry [16, 17], among others.

Various other studies have been performed with strong light-matter coupling, e.g. 2D spectroscopy of polaritonic states [18], vibropolaritonic infrared (IR) emission [19], optomechanical coupling in picocavities [20], Bose-Einstein condensation [21], single-molecule emission in plasmonic nanocavities [22], the strong light-matter interaction in hybrid nanostructures [23], carrier dynamics in plasmonic nanoparticles [24], and coherent emission with surface plasmons [25], to mention a few.

Strong light-matter coupling has now been realized for a wide range of systems, from single emitters in plasmonic cavities [26], photonic crystals [27], plasmonic nanocavities [28], superconducting circuits [29], single open plasmonic nanocavities [30], to liquid phases [31, 32], living bacteria [33, 34], light-harvesting complexes [35], quantum dots [36], organic dyes [37], surface-plasmon polaritons and molecular vibrations [38], diamond color centers [39], and many others.

To understand these intriguing effects observed in recent experiments, numerous theoretical studies have already been performed. In this article, we review these theoretical studies, as well as the aforementioned experimental studies, with a particular emphasis on the two very active and now rapidly converging routes to use strong light-matter interactions, i.e. single-molecule strong coupling using highly confined nanoplasmonic modes and collective strong coupling in polaritonic chemistry in optical cavities as summarized in Figure 1. With this unified perspective, this review article complements the already existing reviews in this field (such as Ref. [5] on experimental progress in polaritonic chemistry, Ref. [40] on novel spectroscopies, Refs. [41, 42] on theoretical progress in polaritonic chemistry, or Ref. [43] on ultra-strong coupling).

The article is structured as follows: we start by providing a general overview of light-matter interactions and describing the conditions under which the light-matter interaction can enter the strong, ultra-strong, or deep-strong coupling regimes. Next, we discuss the few-emitter coupling in nanoplasmonics and the strong coupling in collective strong coupling and review the theories of quantum

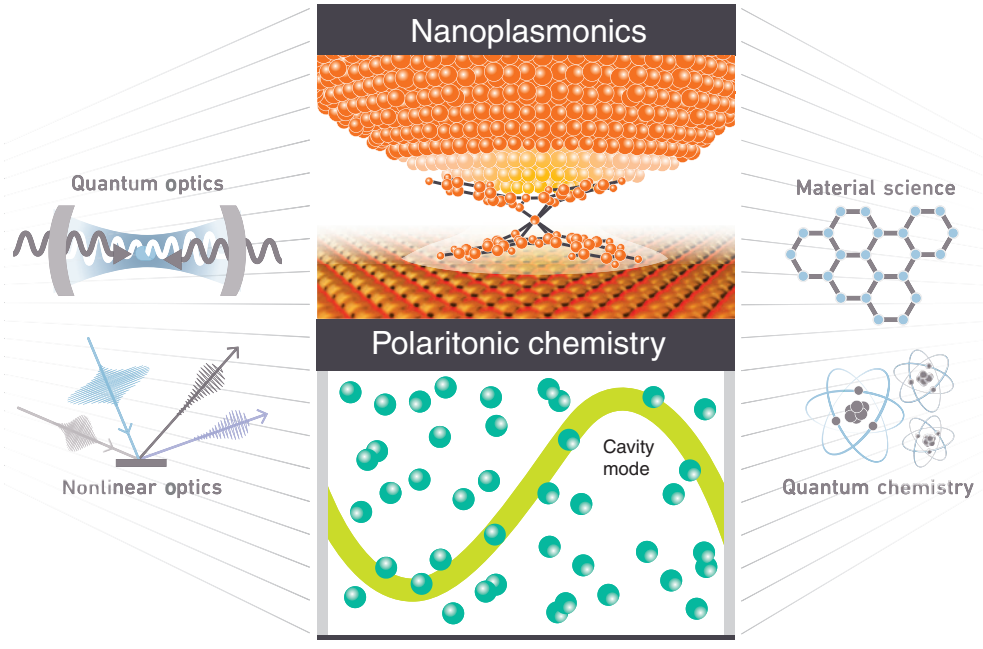

Figure 1: Nanoplasmonic structures as well as polaritonic chemistry use strong light-matter interactions. Both fields benefit from generalized methods from more established fields, such as *ab initio* materials science, quantum chemistry, quantum optics, and nonlinear optics, among others. Our review discusses this exciting intersection of fields and presents recent results in polaritonic chemistry and quantum optics at the atomic scale from a theoretical and computational perspective.

electrodynamical density functional theory (QEDFT) and cavity Born-Oppenheimer approximation (CBOA). Finally, we discuss the perspectives and a roadmap for the field to explore new quantum effects in cavity-correlated dynamics.

2 Basic heuristics of strong coupling

In this section, we first start by reviewing the basic Hamiltonian description of the interaction between light and matter and delineating the differences among weak coupling, strong coupling, and ultra-strong coupling. Then, we describe when light-matter interactions enter the strong coupling regime in a range of matter and photon systems. For the matter, we consider both single-molecule and many-molecule ensembles; for the photon, we consider single-mode, multimode, and continuum-mode photonic systems.

2.1 Quantum theory of photon-emitter interaction

We start by briefly discussing the light-matter interaction in the nonrelativistic limit [44–48]. For a system of nonrelativistic charges, the light-matter interaction Hamiltonian can be introduced by the minimal coupling principle in Coulomb gauge [48] ($\hat{\mathbf{p}}_i \rightarrow \hat{\mathbf{p}}_i - e\hat{\mathbf{A}}(\mathbf{r}_i)$), where $\hat{\mathbf{p}}_i$ is the momentum of the particle i and the vector potential of the electromagnetic field is denoted by $\hat{\mathbf{A}}$. This gauge is also called the "momentum gauge". In an alternative representation, the "multipole representation" or "length gauge", the interaction is formulated in terms of electric displacement and magnetic fields $\hat{\mathbf{D}}(\mathbf{r})$ and $\hat{\mathbf{B}}(\mathbf{r})$ coupling to the matter quantities, which are the polarization $\hat{\mathbf{P}}(\mathbf{r})$ and the magnetization density $\hat{\mathbf{M}}(\mathbf{r})$, respectively [48].

In the dipole approximation where the wavelength of the photon is much longer than the physical extent of the system of charges, only the lowest-order multipole moment of the polarization $\hat{\mathbf{P}}$, i.e. the dipole moment $\hat{\boldsymbol{\mu}} = -e\sum_{i=1}^{N}\hat{\mathbf{r}}_i$ for N electrons, is considered. Here, the interaction Hamiltonian $\hat{H}_{\text{int}}$ between light and matter takes the following explicit form [48]:

$$\hat{H}_{\text{int}} = \hat{\boldsymbol{\mu}} \cdot \hat{\mathbf{D}}(\mathbf{r}_0)/\varepsilon_0 + \hat{\varepsilon}_{\text{dip}}, \tag{1}$$

where the electric displacement field operator $\hat{\mathbf{D}}$ is evaluated at the center of charge $\mathbf{r}_0$. In Eq. (1), $\hat{\varepsilon}_{\text{dip}}$ is a dipole self-energy term that appears as a result of the canonical transformation from the momentum gauge to the length gauge and emerges only in a fully quantum analysis of light-matter interactions in which the electromagnetic field is quantized [47, 49]. The dipole self-energy term does not contain photon creation and annihilation operators. Although this term does not play a direct role in emission and absorption processes due to the lack of photon operators, it has important consequences when considering energy shifts and nonperturbative phenomena. We refer the reader to Refs. [32, 36, 49, 50] for more details on this subtle discussion.

To analyze strong light-matter coupling, we consider a single molecule interacting with a low-loss single-mode optical cavity. Physically, this is realized by having a molecular transition being nearly on-resonance with a particular cavity mode. In the case where the optical modes are of low (but nonzero) loss, the electric displacement field operator $\hat{\mathbf{D}}(\mathbf{r})$ of the single-mode field can be expressed in terms of a normalized cavity mode $\mathbf{F}(\mathbf{r})$ and a photon annihilation (creation) operator $\hat{a}^{(\dagger)}$ as [45]

$$\hat{\mathbf{D}}(\mathbf{r}) = i\varepsilon_0 \int d\omega \rho(\omega) \sqrt{\frac{\hbar\omega}{2\varepsilon_0 V}} (\mathbf{F}(\mathbf{r})\hat{a}(\omega) - \mathbf{F}^*(\mathbf{r})\hat{a}^\dagger(\omega)), \tag{2}$$

where V denotes the mode volume of the cavity, i.e. the effective amount of space of the cavity mode. In general, a cavity mode is broadened by losses as expressed by a density of states, typically taken as Lorentzian function $\rho(\omega) = \frac{1}{\pi}\frac{\kappa/2}{(\omega-\omega_c)^2 + (\kappa/2)^2}$, where κ is the photon dissipation rate and ω_c is the central frequency of the cavity mode. The prefactor $\sqrt{\frac{\hbar\omega}{2\varepsilon_0 V}}$ in Eq. (2) is the electric field of a single photon. It is equal to the root mean square of the quantized electric field in the electromagnetic vacuum and thus represents the strength of the quantum-fluctuating electric field that couples to an emitter.

Further, in the limit of a very low-loss cavity, much narrower than any relevant emitter linewidths, one usually replaces $\rho(\omega)$ with $\delta(\omega - \omega_c)$, writing the field operator in terms of a single mode. By emitter linewidth, we mean the full-width at half-maximum of the density of states of excited state in question. It is this single-mode expression that is used in the famous Rabi model [51, 52]. In the Rabi model, the matter part is described by a two-level system with the electronic ground state $|g\rangle$, the electronic excited state $|e\rangle$, and the electronic excitation energy ω_a. This two-level system is coupled to a single-cavity mode of frequency ω_c. The Rabi model takes the following form including the Rabi frequency Ω:

$$H_R = \frac{1}{2}\hbar\omega_a\hat{\sigma}_z + \hbar\omega_c\hat{a}^\dagger\hat{a} + \hbar\Omega(\hat{a}+\hat{a}^\dagger)\hat{\sigma}_x, \quad (3)$$

where $\hat{\sigma}_x$ and $\hat{\sigma}_z$ are Pauli matrices, respectively. The Rabi model of Eq. (3) does not contain the dipolar self-energy $\hat{\varepsilon}_{\text{dip}}$ of Eq. (1), as this term takes the form of a constant for a two-site model. We note that only recently an analytical solution to the Rabi model was found [53].

By adopting the rotating wave approximation, which neglects nonresonant terms in the interaction Hamiltonian of Eq. (3), we recover the Jaynes-Cummings model [54, 55]. The Jaynes-Cummings model can be analytically solved and thus has heavily contributed to the understanding of the fundamental nature of the light-matter interaction, e.g. see Ref. [55] and the references therein. In the Jaynes-Cummings model, the Rabi splitting, i.e. the splitting between the lower and upper polariton branches, is directly connected to the Rabi frequency and is given by 2Ω. We will discuss the magnitude of the Rabi frequency in the following.

2.2 When is light-matter coupling strong or ultra-strong?

An important quantity in characterizing the coupling between light and matter is the Rabi frequency Ω that enters the Rabi model of Eq. (3) and is defined by [9, 56]

$$\Omega = \frac{\mu}{\hbar}\sqrt{\frac{\hbar\omega}{2\varepsilon_0 V}} \quad (4)$$

The Rabi frequency contains the dipole moment μ of the particular electronic transition that forms the two-level system in the Rabi model and is proportional to the root-mean-square electric field of a single photon that effectively drives the molecule to interact with light.

In the wide field of light-matter interactions, the term "strong coupling" is usually used for two distinct situations. In one situation, the term refers to the situation where the cavity is of high enough quality such that the two-level system can emit and reabsorb a photon several times before it is irreversibly lost to the environment. Only if this is the case, experiments are able to clearly resolve the Rabi splitting in spectroscopic measurements. In another usage of the phrase, "strong coupling" sometimes refers to situations where Rabi splitting is so strong that the rotating wave approximation used to derive the Jaynes-Cummings model is not applicable anymore. This regime is commonly referred to as the ultra-strong or deep-strong coupling regime depending on the precise magnitude strength of the coupling between light and matter. We start by discussing the first situation and then analyzing the latter meaning.

Before going into details, we first mention a useful criterion from Ref. [47] regarding when the coupling of light and matter is strong between a discrete emitter state and a continuum of photonic modes. In Complement C_{III} of Chapter 3, the authors considered a discrete state coupled to a continuum of photon modes with width w_0, which represents the bandwidth of photon frequencies that interact with the emitter. In that chapter, the authors noted that when the calculated decay rate of the emitter Γ is much smaller than the width w_0, i.e. $\Gamma \ll w_0$ the dynamics of the combined system are well described by weak coupling exponential decay dynamics. In the opposite limit, $\Gamma \gg w_0$, the continuum looks like a discrete state to the emitter, and Rabi oscillations occur. We now show that this criterion allows to understand when strong coupling arises.

For "small" values of the Rabi frequency Ω, such that the (enhanced) linewidth of the emitter is much smaller than the cavity linewidth κ, the single-cavity mode appears to the emitter as a broad continuum, and the dynamics of an excited emitter is irreversible emission into cavity modes. Note that the "continuum" of photon frequencies seen by the emitter is represented by the continuous set of frequencies in which the density of states of the cavity mode is not negligible. For a cavity with a Lorentzian density of states, the decay rate κ of the cavity mode represents the bandwidth of the continuum. In this weakly coupled limit, the decay dynamics are well described by a first-order perturbation theory calculation of transition amplitudes from the state $|e, 0\rangle$ to $|g, \omega\rangle$, where ω is a frequency in the support of the cavity density of states.

In this case, the rate of decay is given by Fermi's Golden Rule, as expected when considering the dynamics of a discrete level coupled to a continuum. Performing this calculation, one finds that the rate of emission of a cavity photon by a molecule is given by $\Gamma = \frac{4\Omega^2}{\kappa}$ [57]. Expressing Ω in terms of the dipole moment, photon frequency, and photon mode volume, one finds that the rate of decay $\Gamma = F_p\Gamma_0$, where $F_p = \frac{3}{4\pi^2}\frac{Q}{n^3V/\lambda_p^3}$, is the famous Purcell factor [58]. In this formula, $Q = \frac{\omega_c}{\kappa}$ is the quality factor or Q factor of the cavity mode, whereas $\lambda_p = \frac{2\pi c}{\omega}$ is the photon wavelength, n is the index of refraction occupying the cavity, and V is the volume of the cavity mode. The main assumption in this formula is that the emitter line

is concentric with the cavity line and that the emitter line is much narrower. We additionally note that if the free-space emitter linewidth is already much wider than the cavity linewidth (because the cavity is extremely low loss or the emitter is broadened by another mechanism such as Doppler or inhomogeneous broadening), the emitter will also be in a regime of weak coupling, as excitations are lost into the far field much faster than the emitter can interact with the cavity.

We refer to the "strong coupling" regime as the regime where the light-matter interaction is strong enough such that emitter coherently interacts with the cavity and can emit and reabsorb cavity photons to undergo Rabi oscillations between excited and ground states several times before the cavity photon is lost or before emission happens into the far field.

Physically, this regime, provided that $\Gamma \gg \Gamma_0$ (where Γ_0 is the bare emitter decay rate), as is typically the case in strong coupling, should coincide with $\Gamma \geq \kappa$, as expected from the criterion presented in Ref. [47]. From the expression $\Gamma \sim \Omega^2/\kappa$, one has that the onset of strong coupling should coincide with $\Omega \geq \kappa$. Strictly speaking, it is inconsistent to use a weak coupling result to determine the strong coupling condition. However, as the condition $\Gamma \sim \kappa$ represents the case where the emitter and cavity linewidths match, invalidating irreversibility and weak coupling, one should expect this to be the regime where strong coupling sets in. Thus, to summarize, one is well into the strong coupling when $\Omega \gg \kappa$ and $\Omega \gg \Gamma_0$. The transition to the strong coupling regime is when the upper and lower polariton lines are clearly spectroscopically resolvable. This occurs when the coupling $\Omega > \frac{1}{\sqrt{2}}\sqrt{\kappa^2 + \Gamma^2}$, as described in the review by Torma and Barnes [59], models the strong coupling as a coupled oscillator problem.

Historically, this was the first regime of strong coupling theoretically considered and experimentally observed in both few-emitter and collective contexts [21, 60–66]. Theoretically, the dynamics of the molecule in a cavity in this strong coupling regime is well described by a simple Jaynes-Cummings model provided that the Rabi oscillations are much slower than the cavity frequency and the rotating wave approximation is applicable [54, 55].

The second comparison $\Omega \geq \omega_c$ corresponds to a breakdown of the rotating wave approximation. This regime is also called the ultra-strong or deep-strong coupling regime [67, 68] and has been experimentally accessed in few-emitter systems only recently in the context of circuit QED systems [69–71]. The term "ultra-strong coupling" has been taken by several authors to mean $\Omega/\omega_c \geq 0.1$, whereas "deep-strong coupling" refers to $\Omega/\omega \geq 1$ [67].

In the above, we have implicitly assumed that only a single emitter is coupled to the cavity mode. If an ensemble of N emitters is coupled to the cavity, the Rabi model can be extended to the so-called Dicke model [72, 73]. In the Dicke model, the effective coupling constant (with dimensions of frequency) scales as $\Omega_{\text{eff}} = \sqrt{N}\Omega$. This square-root scaling with the number of emitters can lead to a very large enhancement of the coupling constant for a large number emitters [6], thus allowing experimentalists to avoid creating either very low-loss or very low mode-volume cavities.

We now discuss one more interesting possibility for strong coupling: strong coupling of an emitter to a continuum of photonic modes. On the one hand, as strong coupling appears to be related to reversibility, and a continuum of modes appears to imply irreversible coupling, the answer would appear to be that it is not possible to have strong coupling to a continuum of photonic modes. On the other hand, the strong coupling condition $\Omega \gg \kappa$ (or $\Gamma \gg \kappa$) says that the condition for strong coupling is that the enhanced linewidth of the emitter is large compared to the frequency scale at which the photonic density of states varies. Thus, it should be possible, and in fact, this possibility has been considered theoretically in earlier works via a Laplace transform formalism [74]. Moreover, there are now recent experiments that study the coupling of superconducting qubits to a continuum of transmission line modes in the regime where the emission rate exceeds the transition frequency [29]. In general, it is currently understood that a useful criterion for the possibility of continuum ultra-strong coupling is that the spontaneous emission rate calculated from Fermi's Golden Rule is comparable to the transition frequency, as this is when the rotating wave approximation breaks down [47].

2.3 Quantifying strong coupling

To conclude this section, we provide some estimates for dimensionless coupling constants of the form for different classes of systems. In general, recent developments in the field we review have focused on ultra-strong coupling as opposed to strong coupling. As a result, we focus on ultra-strong coupling constants. In estimates 1–3, the emitter we considered is coupled to a continuum of modes, so we must compare the enhanced decay rate either to the bandwidth of the continuum, if there is one, or the emitter frequency itself, the latter of which signals a breakdown of the rotating wave approximation. The decay rate is the natural choice for the numerator, as a Rabi frequency is typically not considered when coupling to a continuum.

In estimate 4, we look at a single emitter in a cavity and estimate the strong and ultra-strong coupling constants to show that the condition for ultra-strong coupling is much more stringent even when one is well into the strong coupling regime. In estimates 5 and 6, we look at ensembles of emitters coupled to a common cavity mode and look at the ultra-strong coupling constant, comparing the Rabi frequency to the cavity frequency, to gauge the breakdown of the rotating wave approximation.

1. Hydrogen 2p to 1s transition: The rate of this transition is 6.25×10^{8} s^{-1} and the natural frequency is given by 1.55×10^{16} rad/s. As a consequence, the effective coupling constant in this case would be $\sqrt{\frac{6.25\times10^{8}}{1.55\times10^{16}}}\approx2\times10^{-4}$. This transition is well into the regime of weak coupling [75].
2. A dye molecule with a radiative transition frequency of 600 nm with a free-space emission lifetime of 10 ns experiencing a Purcell enhancement of 1000 due a plasmonic cavity, as recently shown in Ref. [76]. In that case, the coupling constant is approximately 0.006, still far into the weak coupling regime.
3. IR Rydberg-like 7500 nm transition between the 6p and 5s levels of a hydrogen atom coupled to highly confined phonon polaritons in a material such that the Purcell factor is on the order of 10^{6} [77]. Further assume that the initial decay rate is $\Gamma=10^{6}$ s^{-1}. In that case, the coupling constant defined by Γ/ω_0 is on the order of 0.06. However, in the specific case of phonon polaritons, the spectral band at which surface phonon polariton modes exist is narrow, about 1/10 of the transition frequency. In this case, the denominator of the coupling constant, which should represent the frequency bandwidth of the photonic density of states, should be about a factor of 10 smaller, making the coupling constant more like 0.2. In this case, it could be possible to observe substantial corrections to the weak coupling dynamics. Interestingly, this suggests that large dipole moment transitions in the IR, where high optical confinement and low losses are possible, are an almost ideal parameter range for strong coupling physics.
4. GaAs quantum dot with a 744 nm transition coupled to a photonic microcavity with a quality factor of 12.000 and a mode volume of 0.07 μm^3: The coupling constant for conventional cavity strong coupling of Ω/κ is about 2. On the contrary, the coupling constant defined by Ω/ω_0 is on the order of 0.02. This shows that the conditions for cavity strong coupling are much less stringent than the conditions for ultra-strong coupling and the breakdown of the rotating wave approximation [64].
5. For molecular liquids that are strongly coupled to multiple IR cavity modes, the collective coupling constant $\Omega/\omega=0.24$ has been reached in Ref. [32].
6. Consider a stack of quantum wells (QWs) collectively coupled to a metallic cavity as in Ref. [36]. For the case of a stack of 25 QWs of width 32 nm with a first excited-state energy of 12 meV, the collective coupling constant Ω/ω is 0.48.

3 Few-emitter strong coupling in nanoplasmonics

In this section, we review, from a theory-driven approach, strong light-matter interactions with one or few emitters interacting with highly confined plasmonic modes. As discussed in Section 2, the rate of emission into the electromagnetic field goes as $\Omega^2/\kappa\sim(Q/(n^3V/\lambda_p^3))\Gamma_0$ [58], where $\lambda_p=\frac{2\pi c}{\omega}$ is the wavelength of a photon in vacuum at the same frequency and Γ_0 is the free-space decay rate of the emitter. As a result, despite the high losses of plasmons in nanocavities, they can facilitate strong light-matter interactions by virtue of their small mode volumes compared to the "photon volume" $\sim\lambda_p^3$. Recent experiments in plasmonics and phononics have shown that light can be confined to anywhere between $(10^{-5}-10^{-9})\lambda_p^3$ [3, 28, 78, 79]. This has been demonstrated at visible frequencies using gold nanogaps [28], in the mid-IR using plasmons in unstructured graphene [79], graphene-hBN-gold structures [3], and also phonon-polaritons in structured and unstructured polar dielectrics such as silicon carbide and hBN [80–82].

In Figure 2, we show two recent experiments that demonstrate the promise of plasmonics for inducing strong light-matter interactions. Figure 2A–F show the main results of an experiment by Akselrod et al. [76], which measured the time-resolved fluorescence (Figure 2E) an ensemble ruthenium metal-complex dye molecules placed in a 5–15 nm nanogap between a Ag nanocube and a gold film (Figure 2B). With such a "nanoparticle on mirror" (NPoM) geometry, the authors were able to demonstrate a maximum spontaneous emission rate enhancement of 860. Perhaps more importantly accounting for material losses, the line shape of the molecular fluorescence (Figure 2A), the distribution of emitters in the nanogap (Figure 2C), and the extreme inhomogeneity of the nanogap mode, the authors achieved a very good agreement between classical electromagnetic simulations and experimental results (Figure 2F), demonstrating the validity of the Purcell

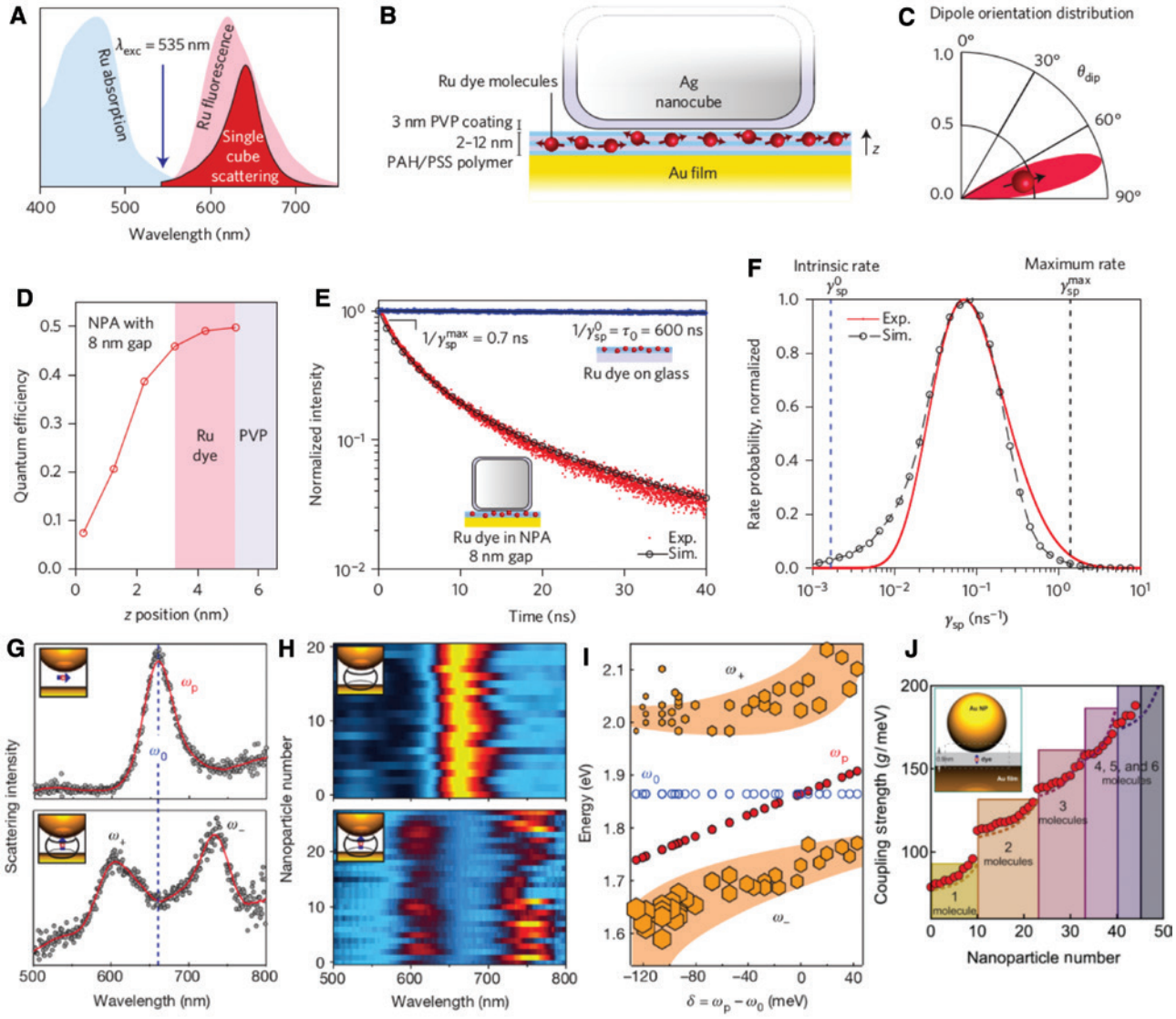

Figure 2: Strong Purcell effects and few-molecule strong coupling via plasmonic nanocavities.
(Top) Experimental results [76] showing the strong enhancement of spontaneous decay by dye molecules in a nanogap between a Ag nanocube and a gold film (B). Due to the nanoscopic mode volume of the nanocube film mode, the spontaneous enhancement of dipoles inside the nanogap can be enhanced by as much as a factor of 1000 (E). Taking into account the distribution of emitters in position and orientation (C) along with the nanoparticle and molecule line shapes (A), the authors achieved good agreement between the theory of the Purcell effect and experiments (F). (Bottom) Experimental results [28] showing the strong coupling regime in the interaction of molecules with a NPoM mode with a gap of 0.9 nm (G). By measuring the scattering of light from the system of molecules + NPoM, the authors observed a strong Rabi splitting associated with the formation of coupled excitations of plasmons and molecules (H). By increasing the number of molecules to 10, the resulting collective coupling allows the strong coupling regime to be achieved (I). (A–F) Adapted with permission from Ref. [76] (© 2014 Springer Nature). (G–J) Adapted with permission from Ref. [28] (© 2016 Springer Nature).

effect theory in plasmonic nanostructures. It also demonstrates the promise of NPoM geometries for achieving strong light-matter coupling. In fact, in another recent experiment by Chikkaraddy et al. [28], this NPoM geometry was taken to the extreme nanoscopic limit, featuring a gap size of 0.9 nm (Figure 2G). By measuring the scattering spectra of methylene blue encapsulated in Cucurbit[7]uril "barrels", the authors were able to observe Rabi splittings on the order of 90 meV compared to a plasmon dissipation rate of about 120 meV, causing the system to be in the strong coupling regime (Figure 2H). By including a few more molecules into the system (Figure 2I), they can make use of the $\sqrt{N}$ enhancement of the coupling constant to place the system well into the strong coupling regime.

In what follows, we give a brief theoretical overview of what theory tools are needed to analyze plasmon-enhanced light-matter interactions. From there, we will discuss some of the important new physics that arises when the mode volume of light is decreased to the scale of a few cubic nanometers.

3.1 Theoretical tools for strong plasmon-enhanced light-matter interactions

We now move to a theoretical description regarding the interactions between emitters and plasmonic systems, such as nanoplasmonic cavities, thin films, or much more complicated geometries. To understand the coarse features of the experiments discussed above, one can largely follow the approach of Section 2: quantize the field of the plasmons by expanding the electric field in properly normalized plasmon modes $\mathbf{F}(\mathbf{r})$ and normalizing them such that the energy in the plasmonic mode is equal to $\hbar\omega$. However, such an approach is only strictly valid for very low-loss modes, although reasonable agreement with a more complex theory incorporating losses can be achieved even when the modes have a quality factor as low as 5 [83]. Incorporating losses introduces complications because, in the extreme near field of a lossy material, large deviations can arise from the single-mode picture depicted in Eq. (3) arising effectively from interactions in which an emitters dipole induces dipoles in a highly polarizable (conductive or lossy) material and transfers energy to the material dipoles. It turns out that the analysis of light-matter interactions for highly lossy materials is possible and falls under the so-called "macroscopic QED formalism". Although we do not derive the basic formalism here, leaving that to dedicated reviews on the formalism such as Refs. [84, 85], we can quickly make the basic results plausible.

One reason for the failure of a mode expansion approach when losses are appreciable is that the completeness and orthonormality of the eigenmodes no longer necessarily hold. This is a known issue not just in light-matter interactions but simply classical electromagnetism, where convenient approaches based on modes fail when losses are present [86]. In that domain of classical electrodynamics, one can still understand the dynamics of fields and electromagnetic resonances through the dyadic Green's function of the system [87], defined formally via $\mathbf{G}(\mathbf{r}, \mathbf{r}', \omega) \equiv \left(\nabla \times \nabla - \varepsilon(\mathbf{r}, \omega) \frac{\omega^2}{c^2} \right)^{-1} \delta(\mathbf{r} - \mathbf{r}') I_3$. From the dyadic Green's function of the system, one can calculate the fields induced by an arbitrary arrangement of electric currents (equivalently, an arbitrary arrangement of electric dipoles). The real-valued electric field associated with an arbitrary arrangement of dipoles with spectrum $\mathbf{j}(\mathbf{r}, \omega)$ is given by $\frac{1}{2}\int d\omega\omega \int d\mathbf{r}' i\omega\mu_0 G(\mathbf{r}, \mathbf{r}', \omega)\mathbf{j}(\mathbf{r}', \omega)e^{-i\omega t} - c.c.$ It stands to reason that, if the current density in a material at a given point in space, at a given frequency, and in a given direction can be considered as an elementary excitation of a field, which in this case is a polarization field, then the electromagnetic field can be quantized in terms of these current operators and the classical dyadic Green's function. This assumption is the essence of the macroscopic QED method. Following canonical commutation relations for the currents based on the linear response theory and the fluctuation-dissipation theorem (see Ref. [85]), the Schrödinger picture ($t = 0$) quantized electric displacement field operator can be written as

$$\hat{\mathbf{D}}(\mathbf{r}) = i\varepsilon_0 \int d\mathbf{r}' d\omega \sqrt{\frac{\hbar}{\pi\varepsilon_0}} \sqrt{\mathrm{Im}\,\varepsilon(\mathbf{r}', \omega)} (\mathbf{G}(\mathbf{r}, \mathbf{r}', \omega)\hat{\mathbf{f}}(\mathbf{r}', \omega) - h.c.). \quad (5)$$

In this expression, the $\hat{\mathbf{f}}$ operators are rescaled dipole operators such that they satisfy canonical commutation relations: $[\hat{f}_i(\mathbf{r}, \omega), \hat{f}_j^\dagger(\mathbf{r}', \omega')] = \delta(\mathbf{r} - \mathbf{r}')\delta(\omega - \omega')\delta_{ij}$ and $\varepsilon(\mathbf{r}, \omega)$ is the dielectric function, which relates the macroscopic polarization to macroscopic electric fields. As in the "low-loss" case, the coupling Hamiltonian between an emitter and a lossy material in the long-wavelength approximation is the dipole Hamiltonian of Eq. (1). A key result from this formalism is that, if one computes the rate of spontaneous emission of material dipoles (anywhere in the material and in any direction) by an emitter of natural frequency ω_0, the spontaneous emission rate follows as [88]

$$\Gamma = \frac{2\mu_0}{\hbar}\omega^2 \boldsymbol{\mu}^* \cdot \mathrm{Im}\,\mathbf{G}(\mathbf{r}, \mathbf{r}, \omega_0) \cdot \boldsymbol{\mu}. \quad (6)$$

This expression leads to a Purcell factor for an emitter with an $\hat{n}$-directed dipole moment of magnitude $\frac{6\pi c}{\omega}\hat{n} \cdot \mathrm{Im}\,\mathbf{G}(\mathbf{r}, \mathbf{r}, \omega_0) \cdot \hat{n}$. Because, as discussed in Section 2, the emission rate, compared to a photon dissipation rate, can be used as a proxy for a coupling constant, in experimental work, this expression for Γ is commonly used to assess whether or not the strong coupling regime is reached. This was done in the experiment on strong coupling to a plasmonic mode. Thus, the calculation of the Green's function of an optical structure allows to quantitatively assess plasmon-enhanced decay rates and evaluate whether the strong coupling regime was reached.

The Green's function is determined by the dielectric function $\varepsilon(\mathbf{r}, \omega)$ (currently assumed to be spatially local); thus, finding the Green's function $\mathbf{G}(\mathbf{r}, \mathbf{r}, \omega)$ boils down to finding the electric field at position $\mathbf{r}$ created by a dipole at position $\mathbf{r}$ and frequency ω, which is a classical electromagnetic problem. In the domain where the emitter is more than roughly 20 nm from the surface of the plasmonic cavity, and in the domain where the plasmonic cavity can be described by a local dielectric function, the relevant Green's function can be calculated using standard numerical algorithms for solving Maxwell's equations such as finite-difference time-domain (FDTD) methods [89] or boundary element methods [90]. These methods are applied in recent experiments such as those discussed above, both assuming a spatially local dielectric function for the NPoM [28, 76].

It is now well known experimentally [78, 91–94] that for metal nanoparticles with sizes below 10 nm, nanoscopic metallic gaps, and very high wavevector plasmons such as in plasmonic film geometries, the effects of spatial dispersion become relevant and the electromagnetism must now be described by the nonlocal permittivity $\varepsilon(\mathbf{r}, \mathbf{r}', \omega)$. In general, these effects are relevant once the spatial scale of the electromagnetic field variation is comparable to the Fermi wavelength of the underlying metal. Phrased differently, it matters when the momentum components of the electromagnetic field are comparable to the momentum of electrons in the underlying metal. It is in this regime that plasmons can, for example, induce strong nonvertical interband transitions in the underlying metal, allowing for an increased phase space of plasmon damping and lower plasmon lifetimes [95–98]. Although this review is not dedicated to the treatment of nonlocality, leaving that for more comprehensive reviews such as Refs. [99–103], we note that there are many ways to treat nonlocality in metals, from hydrodynamic models [100] to Feibelman d-parameter approaches [104, 105] with input from time-dependent DFT (TDDFT) [103]. In any of these, once the dielectric function is known and the Green's function is computed, it turns out that Eq. (6) still holds, but with the Green's function that accounts for nonlocality. By and large, the effect of nonlocality on spontaneous emission enhancements is to reduce them due to increased damping that invariably comes with spatial nonlocality.

3.2 Novel light-matter coupling phenomena at the extreme nanoscale

In the rest of this section, we discuss systems that fall outside common treatments of emitter-plasmon interactions. In particular, we discuss methods that become relevant when the electromagnetic energy is confined to scales comparable to the length scale of an emitter. One reason to expect the physics of emission to change when electromagnetic fields are highly confined is hinted by the common treatment of emitters as dipoles. In principle, the emitter has to be described by a complicated transition current density determined by the spatial variation of the wave functions participating in the transition. Thus, in principle, it can (and does) have many multipole moments beyond the dipole moment. However, when the emitter is very small compared to the wavelength of light, the dipole component is strongly dominant. The validity of the long-wavelength approximation is given by the parameter [1]

$$ka = \frac{2\pi a}{\lambda}, \tag{7}$$

where k is the wavevector of the optical field, λ is its corresponding wavelength, and a is the "emitter size", which can be roughly parameterized, for example, by the transition multipole moments. In the regime where $ka \ll 1$, the rates of various electric multipolar transitions scale as $\Gamma(En) \sim \alpha(ka)^{2n+1}$, where the terminology "En" denotes a 2^n-pole transition ($n=1$ is dipole, $n=2$ is quadrupole, etc.). Taking $a=1$ nm and a typical free-space wavelength of 1 μm, $(ka)^2 \approx 4\times10^{-5}$, meaning that higher-order transitions become successively slower by this factor, rendering them irrelevant to the vast majority of optical experiments involving emitters.

Taking $a=1$ nm, the optical wavevector k corresponding to a complete breakdown of the dipole approximation is $k=1$ nm^{-1} or $\lambda=6$ nm. These kinds of spatial scales are readily available in recent experiments involving plasmonic Purcell enhancement [76], in single-molecule plasmonic strong coupling [28], and in strong coupling experiments involving "picocavities" [20]. Even for substantially longer wavelengths such as 20 or 30 nm, higher-order multipolar effects can potentially be detected, as discussed in Ref. [83], where it was suggested that graphene plasmons of these wavelengths could already lead to relatively short lifetimes (microseconds) of transitions, which have thus far been spectroscopically unobserved in any experiment such as E4 and E5 transitions, which have typical free-space lifetimes of hundreds and billions of years, respectively. These kinds of effects with higher-order transitions have been considered theoretically in a number of other studies such as [106, 106–113], typically focusing on electric quadrupole and magnetic dipole transitions. Nondipolar effects have also been reported experimentally with larger emitters such as carbon nanotubes [114] and larger quantum dots coupled to plasmonic

nanowires with plasmon wavelengths on the order of 300 nm [115].

That the shrinking of plasmonic wavelengths can lead to normally "forbidden" transitions has been long known. A related fact that is much less appreciated, however, is that the shrinking of the plasmonic wavelength may also lead to extremely high probability of multiplasmon spontaneous emission processes in emitters. Two-photon spontaneous emission by an emitter is a second-order process in quantum electrodynamics that has been known since the 1930s. It was predicted by Goppert-Mayer [116] and subsequently estimated for the hydrogen 2s to 1s transition by Breit and Teller [117]. Being a second-order process in the coupling constant, it scales as $\alpha^2(ka)^4\omega$, in the case where the two-photon transition takes place via two virtual dipole transitions. From this estimation, it follows that two-photon emission is anywhere between 8 and 10 orders of magnitude slower than one-photon emission for atomic emitters in free space. For semiconductor QW-based emitters, the scaling is more favorable, with it having been experimentally determined that the two-photon emission is only five orders of magnitude than one-photon emission [118, 119].

In the presence of a plasmonic environment, analogous to the Purcell effect, the two-photon emission can be greatly enhanced. The theory of plasmon- or cavity-enhanced two-photon emission effects has been worked out in Refs. [77, 83, 120, 121] and has been experimentally supported with the observation of two plasmon-emission rate enhancements of more than 1000 for QW electrons in the vicinity of a bowtie plasmonic antenna. This same theory was used in Ref. [83] to show that, due to the extreme confinement of plasmons in graphene in the IR, atoms could experience two-plasmon Purcell enhancements of more than 10^{10}, leading to emission rates in the microsecond to nanosecond regime. It was also shown that, by combining plasmon confinement with density-of-states engineering, it is also possible to make these two-polariton decays dominant over one-polariton decays by simultaneously having high Purcell enhancement of two-polariton emission frequencies while having only negligible Purcell enhancement at the one-polariton emission frequency [77]. Ultimately, as the spatial confinement of plasmonic modes becomes larger, even without using density-of-states engineering, the multipolariton spontaneous emission processes will have comparable amplitude to the first-order processes, representing the breakdown of the perturbation series and the ultra-strong coupling regime. It is of critical importance to emphasize that the kinds of multiphoton spontaneous emission effects described here are out of the scope of Rabi models that consider either single- or few-photonic modes and also two-level systems. This is for a few reasons: (1) a pair of emitter levels that have a dipole moment is incompatible with two-photon emission as, in the dipole approximation, two-photon transitions preserve parity and (2) two-photon emission rates require knowledge of intermediate emitter states, which is beyond a two-level description. As a result of multiphoton phenomena not being part of the typical theoretical framework, it is interesting to see what role they should play in a description of ultra-strong light-matter coupling.

We conclude this section with an outlook to the future of plasmon-emitter coupling experiments in the extreme-small-wavelength regime. In addition to the experiments by Baumberg et al. demonstrating few-molecule strong coupling to plasmons in nanocavities and picocavities, recent experiments in graphene plasmonics have shown that the mode volume of a plasmon on a graphene-hBN-gold structure can potentially be confined to volumes that are a billion times smaller than that of a photon in free space [3]. A naive estimate of emitter-plasmon coupling suggests that an emitter coupled to such plasmons can be in the ultra-strong coupling regime. This suggests that the regime of ultra-strong coupling of an emitter to a continuum of plasmonic modes is within reach. This regime features a confluence of rich physics such as nondipolar effects, multiphoton effects, quantum nonlocality, and the change of emitter wave functions due to electronic interactions with the nearby plasmonic material. To our knowledge, no theoretical study has considered the confluence of all these effects, and no experimental study has been able to dissect all of these classes of effects. To include all of these effects in a single theoretical model is a formidable challenge due to the need to take into account the following:

1. The detailed shape of the emitter wave function as it becomes very relevant to nondipolar effects;
2. The shape of the emitter wave function as it is affected by the proximity to the plasmonic metal;
3. Nonlocal effects as well as tunneling effects;
4. Potentially large material dissipation, leading to the breakdown of few-mode pictures; and
5. A Hilbert space that has not only many modes (or quasi-modes) but also many potential excitations of these modes as a result of multiphoton interactions.

An interesting testing ground for such a comprehensive theory would naturally be the recent experiments probing the strong coupling of molecule vibrations to "picocavities" [20], formed by the presence of an adsorbed molecule between two metallic facets not even 1 nm apart.

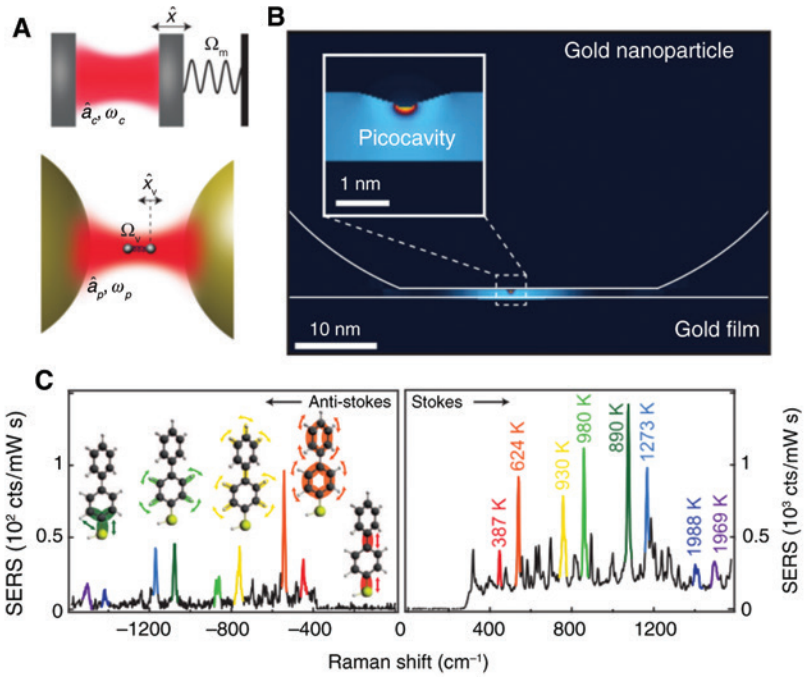

Figure 3: Single-molecule strong coupling in a nanoplasmonics setup.
(A) General setup of a molecular optomechanical system [123]. Between a gold nanoparticle and a gold film, plasmon excitations create hotspots of high field amplitude. (B) Optomechanical coupling of single molecules in picocavities [20]. The shown Raman spectra reveal changes of SERS selection rules. (C) Stokes and Anti-stokes spectra. (A) Adapted with permission from Ref. [123] (© 2015 Springer Nature). (B and C) Adapted with permission from Ref. [20] (© 2016 The American Association for the Advancement of Science).

In this regime, the molecular system can behave as optomechanical systems [122], as shown in Figure 3A, and the picocavity setup is shown in Figure 3B. Benz et al. [20] have demonstrated that the optomechanical coupling of single molecules in picocavities reveals the changes of the surface-enhanced Raman spectroscopy (SERS) selection rules, as shown in Figure 3C.

We note that one emerging theoretical technique for addressing electromagnetic response in subnanometer gaps is that of applying a quantum corrected model (QCM) [101, 124]. The QCM is a phenomenological model in which the gap is modeled as an effectively local material, typically assigned to take the form of a Drude model with a dissipation parameter that is adjustable. Physically, this dissipation rate is meant to reflect the tunneling current between the two sides of the gap. Accordingly, this rate parameter is very large for large gaps, making this effective material very resistive so that tunneling current cannot go through. Similarly, for very small gaps, the dissipation goes to the intrinsic dissipation of the metal region surrounding the gap. Thus, in the limit of zero gap, the model maps to a homogeneous Drude metal model. Notably, this very simple model has had some success in qualitatively explaining the electromagnetic response of gaps at these scales, where the success is determined by direct comparison to TDDFT coupled to Maxwell equations [125].

4 Many-emitter strong coupling in polaritonic chemistry

We devote the remaining part of this article to many-emitter strong coupling and further review the new field of polaritonic chemistry [5]. This new field, where chemical reactions are altered by the strong coupling of light and matter, has seen tremendous experimental advances in recent years. As we have discussed in Section 2, usually in polaritonic chemistry, strong light-matter interaction is achieved by the collective coupling of many chemically active molecules to a single-cavity mode. In this limit, the simplest theoretical description is based on the Dicke model [72, 73], which leads to an effective $\sqrt{N}$ (number of emitters) enhancement of the light-matter coupling strength.

Three representative experiments that exploit the collective strong coupling of many emitters are depicted in Figure 4. The schematic illustration in Figure 4A shows the general setup of an experiment in the field of

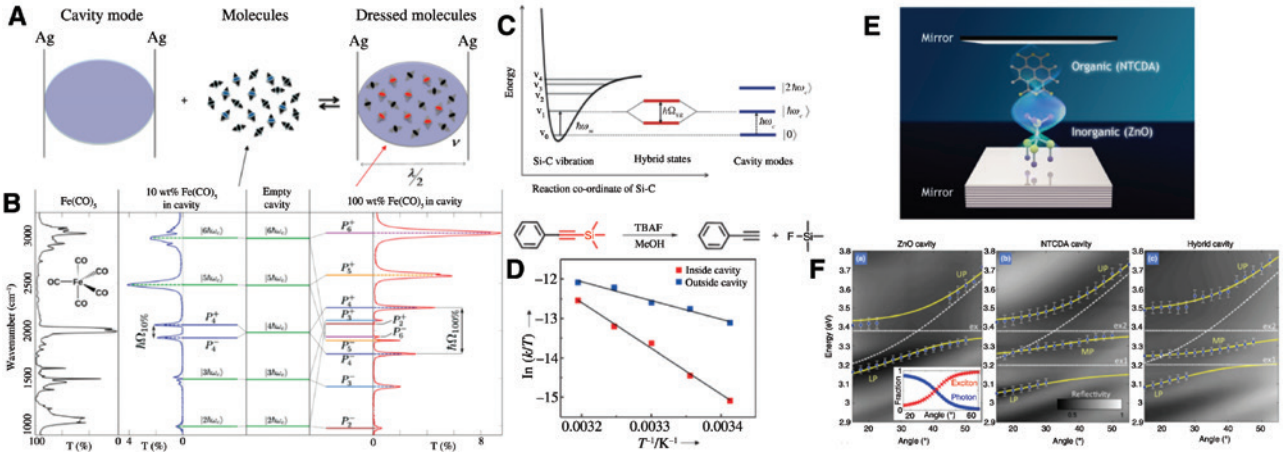

Figure 4: Experiments demonstrating collective strong light-matter coupling.
(A) Adapted with permission from Ref. [123] (© 2015 Springer Nature). (B and C) Adapted with permission from Ref. [20] (© 2016 The American Association for the Advancement of Science). (A) General setup [5] when organic molecules are placed between two Ag mirrors that form an optical cavity to create dressed polaritonic states. (B) Transmission spectrum of such a system. By increasing the density of the $Fe(CO)_5$ compound in the optical cavity, the system shows a transition from the strong (blue) to the ultra-strong (red) coupling limit [32]. (C) Top: Schematic illustration of a strong coupling experiment [8]. The first excitation of an Si-C vibrational mode is strongly coupled to a cavity mode of the same frequency, leading to a Rabi splitting. Bottom: Deprotection reaction of PTA with TBAF. (D) Reaction rate depending on the temperature for reactions inside the cavity (red) and outside the cavity (blue) [8]. (E) Experimental setup [11] of the organic and inorganic molecules that are strongly coupled in a microcavity. (F) Strong light-matter coupling leads to a Frenkel-Wannier-Mott hybridization of excitons [11]. UP, MP, and LP denote the upper, middle, and lower polaritons, respectively. (A) Adapted with permission from Ref. [5] (© 2016 American Chemical Society). (B) Adapted with permission from Ref. [32] (© 2016 American Physical Society). (C and D) Adapted with permission from Ref. [8] (© 2016 John Wiley and Sons). (E and F) Adapted with permission from Ref. [11] (© 2014 American Physical Society).

polaritonic chemistry, where a Fabry-Perot cavity formed by Ag mirrors is used to create cavity modes. Often, the lowest mode is chosen in resonance to a particular molecular transition energy leading to dressed light-matter dressed states with polaritonic character. In Figure 4B, vibrational ultra-strong coupling [32] has been demonstrated. The authors demonstrate that, by increasing the density of $Fe(CO)_5$ in the cavity that has a very strong oscillator strength, due to degenerate CO stretching modes, the light-matter interaction becomes so strong that peaks in the IR spectrum interfere, where the authors report a Rabi splitting up to $\Omega/\omega_c \sim 24\%$. In this novel regime, the light-matter interaction becomes strong enough that the dipole self-interaction $\hat{\varepsilon}_{\mathrm{dip}}$ of Eq. (1) has to be correctly considered to find the correct peak position. In a different experiment, the authors studied the reaction yield of a deprotection reaction. Figure 4C shows the potential energy surface in the Born-Oppenheimer approximation (BOA) along the reaction coordinate. The first excitation of an Si-C vibrational mode is strongly coupled to a cavity mode of the same frequency, leading to a Rabi splitting. The reaction, a deprotection reaction of 1-phenyl-2-trimethylsilylacetylene (PTA) with tetra-n-butylammonium fluoride (TBAF) [8], is depicted in Figure 4C (bottom). Figure 4D then shows the result of that study demonstrating that the rate and yield of chemical reactions can be modified under strong light-matter coupling. The figure shows the reaction rate depending on the temperature for reactions inside the cavity (red) and outside the cavity (blue). Under strong light-matter coupling, the reaction rate is decreased by a factor of up to 5.5, demonstrating the new possibilities in the field of polaritonic chemistry. From the theoretical side, a complete description of this particular experiment still remains elusive and open discussions remain, such as whether the transition state of the chemical reaction inside the cavity is significantly altered under strong light-matter coupling.

In Figure 4E, we depict a different experiment [11] that demonstrates the strong coupling of two degenerate excitons in spatially separated ZnO and 3,4,7,8-napthalene tetracarboxylic dianhydride layers and a cavity mode. This experiment for a hybrid inorganic organic systems demonstrates long-range interactions (>50 nm) far beyond the usual dipole-dipole range (in nanometers) in Figure 4F, as under strong light-matter coupling the dominant length scale becomes the spatial extension of the cavity mode. The long-range behavior of the coupled system originating in the joint coupling of matter with the cavity mode has

also been exploited in other experiments, e.g. for long-range energy transfer [12] and even entanglement [13].

All these intriguing new experiments demonstrate the need to extend current theory methods and even develop new theory methods that treat the matter and light on the same footing. In the following, we review some of the recent theory works.

The nature of these collective polaritonic states emerging in strong light-matter coupling cavities can be analyzed from the standpoint of the Dicke model [72, 73]. In the Dicke model, the electronic excitation in the excited states becomes delocalized [73]. As a consequence, processes that favor delocalization, such as transfer processes, are prime candidates for possible enhancements under strong light-matter coupling. In Ref. [9], a strong enhancement in the charge-carrier mobility for organic semiconductors coupled to a plasmon mode has been reported experimentally. These experiments have been theoretically supported for exciton transfer [126, 127], enhanced electrical polarizability [128], and the modified long-range energy transfer [129–132]. In Ref. [133], it is demonstrated that under strong light-matter coupling the transfer process is not only mediated by the excited state but also that the ground state contributes.

Various other aspects of these new class of experiments have been explained on the theoretical side of polaritonic chemistry, e.g. the possibility to change the pathway of (photo)chemical reactions [134–138], vibrational strong coupling [139–141], and novel collective effects, such as the formation of a "supermolecule" [142] and the optomechanical coupling [143]. Furthermore, new effects in these exciting new limits are the polaritonically enhanced electron-phonon coupling influencing superconductivity [144] or Floquet engineering [145–147].

We would like to review one of such theoretical work more explicitly. In Ref. [134], the authors showed that the new concept of polaritonic surfaces [135] can efficiently explain the suppression of photochemical reactions observed in ultra-strong coupling experiments (Figure 5). Figure 5D shows for a single molecule the wave packet after

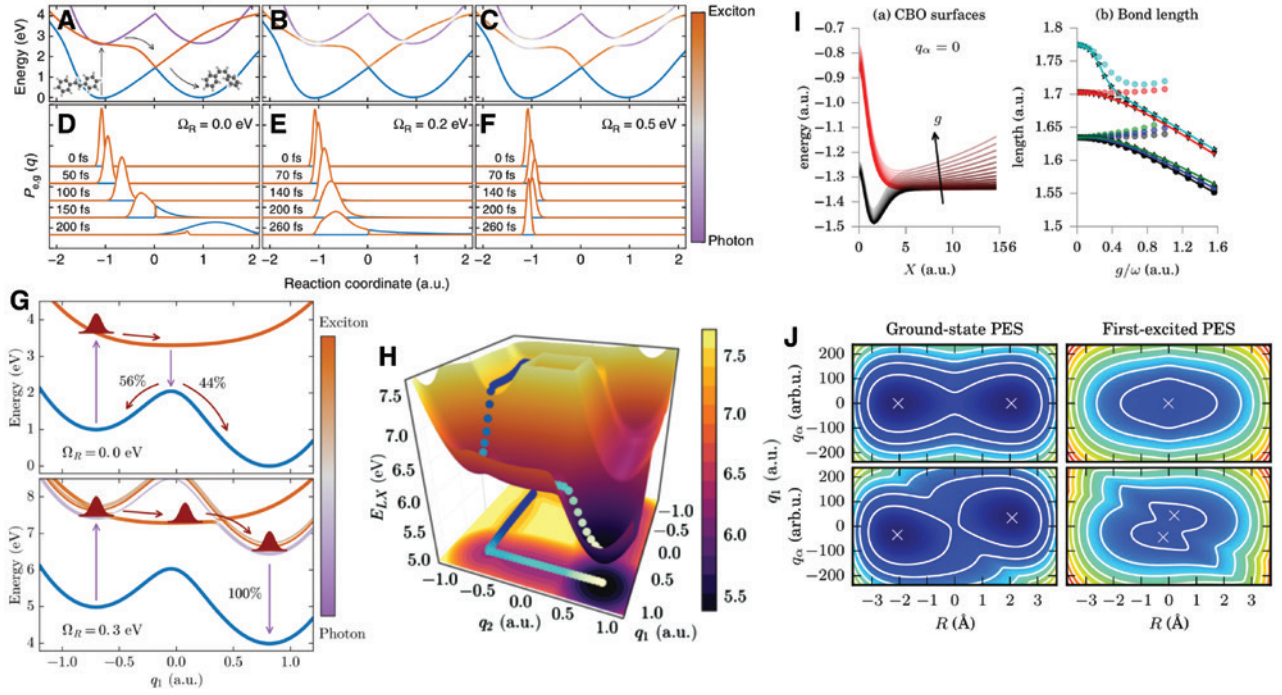

Figure 5: Photochemical reactions under strong light-matter coupling.
(A–C) Suppression of photoisomerization under strong coupling for single molecules [134] with modification of the potential energy surfaces. (D–F) The polaritonic surfaces introduce a energy gap that traps the initially excited-state wave packet. (G) Reaction quantum yield for reaching either the stable (44%) or the metastable (56%) configuration in the electronic ground state can be largely increased in the strong coupling limit [142]. (H) Many-molecule reactions triggered by single photon [142]. (I) Potential energy surfaces in CBOA [50] for a 1D model (a) and changes of the bond length of a hydrogen dimer (b). (J) 2D CBOA potential energy surfaces in weak (top) and strong (bottom) coupling [50]. (A–F) Adapted with permission from Ref. [134]. (G and H) Adapted with permission from Ref. [142] (© 2017 American Physical Society). (I–J) Adapted with permission from Ref. [50].

a Franck-Condon excitation within 200 fs. By increasing the number of considered molecules, Galego et al. found that the excited-state dynamics changes drastically. Within the time frame of 260 fs, the Franck-Condon excited wave packet stays closer to its initial position for stronger Rabi splitting. This behavior is explained in terms of potential energy surfaces. In the case of strong coupling, fractions of the ground-state surface become mixed into the lower polaritonic state that leads to the effective barrier in the excited-state surface. A different setup is shown by the same authors in Ref. [142] as shown in Figure 5G and H. Here, the possibility of single-photon-triggered many-molecule reactions has been analyzed. In the strong coupling regime, the authors found the opening of a new reaction pathway that shows a very high efficiency.

From a chemistry perspective, it is natural to think about how the BOA, a key concept in quantum chemistry, has to be adapted if light and matter strongly interacts. One such extension to the BOA is called CBOA and applicable to study light-matter systems in an optical cavity [50, 148]. CBOA allows to calculate approximate eigenstates of correlated systems containing electronic, nuclear, and photonic degrees of freedom and to interpret dynamical processes in an intuitive way. In this case, the magnetic field of the photon modes can be interpreted as an analogue to the nuclear velocity in real space. With this analogy, whereas the usual BOA is justified by the different time scales of the slower nuclei compared to the faster electrons, CBOA is applicable if the magnetic field in the photon modes is "small" and therefore changes in the electric displacement field occur slowly compared to the electronic degree of freedom due to the Ampére-Maxwell law. As shown in Ref. [148], this is particularly true for eigenstates. The underlying idea of the CBO is to factorize the many-body wave function into electronic and photon-nuclear degrees of freedom. In this case, the wave function can be written as

$$\Psi_i(\underline{\mathbf{r}}, \underline{\mathbf{R}}, \underline{q}) = \sum_{j=1}^{\infty} \chi_{ij}(\underline{\mathbf{R}}, \underline{q}) \psi_j(\underline{\mathbf{r}}, \underline{\mathbf{R}}, \underline{q}), \tag{8}$$

where χ_{ij} is a joint nuclear-photon wave function and ψ_j is an electronic wave function. We show in Figure 5I and J examples for such CBO potential energy surfaces. In Figure 5I, we show for a hydrogen-deuterium dimer in strong coupling [50] how the surface is altered for increasing electron-photon coupling strength. The figure shows the surface along the nuclei distance, and for stronger coupling, the asymptotic behavior changes significantly along this nuclear coordinate. In Figure 5I, we see how we can understand the behavior in more detail. For a Shin-Metiu model [149] in a cavity [50], in the weak coupling limit (upper surfaces), the nuclear and photonic degrees are still approximately separable, but they mix strongly under strong coupling. This mixing leads to a tilting in the 2D joint nuclear-photon surfaces shown in the right. In the strong coupling regime, a new polaritonic degree of freedom emerges [128].

This concept of CBOA can be applied and improved along the lines of standard quantum chemistry approaches, e.g. surface hopping [150] or Car-Parrinello molecular dynamics [151]. There also exist different possibilities to a BOA for correlated electron-nuclear-photon systems; depending how the system is divided, we refer the readers also to Refs. [135, 152].

The field of quantum plasmonics and plasmonic hot carriers is poised to deliver new quantum devices at the boundary of chemistry and quantum optics [153]. Figure 6 shows excited-state electron transfer between faceted metal particles and unoccupied molecular orbitals in adsorbed molecules with angle-resolved excited carrier distribution at the surface of a faceted nanoparticle. Understanding mechanisms for such single-molecule electron transfer in picocavities promises a new era in single-molecule devices.

4.1 QEDFT

As a first step toward a unified *ab initio* description of light-matter coupled systems, recently, different novel and general concepts have been developed. Density-functional theories (DFTs) have played an important role in explaining plasmonic effects, such as ground-state DFT [155] to study the electronic structure of plasmonic resonators or TDDFT [156] to study the dynamical behavior of plasmonic particles [157]. In the original formulation of TDDFT, the electromagnetic field enters via the time-dependent external potential $v_{\text{ext}}(\mathbf{r}, t)$ and thus can, for example, describe the effect of a classical pumping laser field on the system. Typically, such external fields assume the dipole coupling of the electric field to matter, i.e. $v_{\text{ext}}(\mathbf{r}, t) = \mathbf{E}(\mathbf{r}, t) \cdot \hat{\boldsymbol{\mu}}$. To go beyond the dipole approximation, time-dependent current DFT [158] can be used that is based on the electron current $\mathbf{J}$ and an external vector field $\mathbf{A}_{\text{ext}}$ as conjugated variables. To overcome the classical approximation of the electromagnetic field, QEDFT [159–161] can be employed. QEDFT generalizes TDDFT to the realm of correlated electron-photon interactions treating electrons and photons on the same quantized footing. Furthermore, being formulated as an exact reformulation of the combined electron-photon Schrödinger equation, QEDFT is not restricted to few-level approximations as commonly used in quantum optics but allows to study correlated electron-photon dynamics in full real-space. Thus far, QEDFT has been applied to study effective quantum optics systems [161,

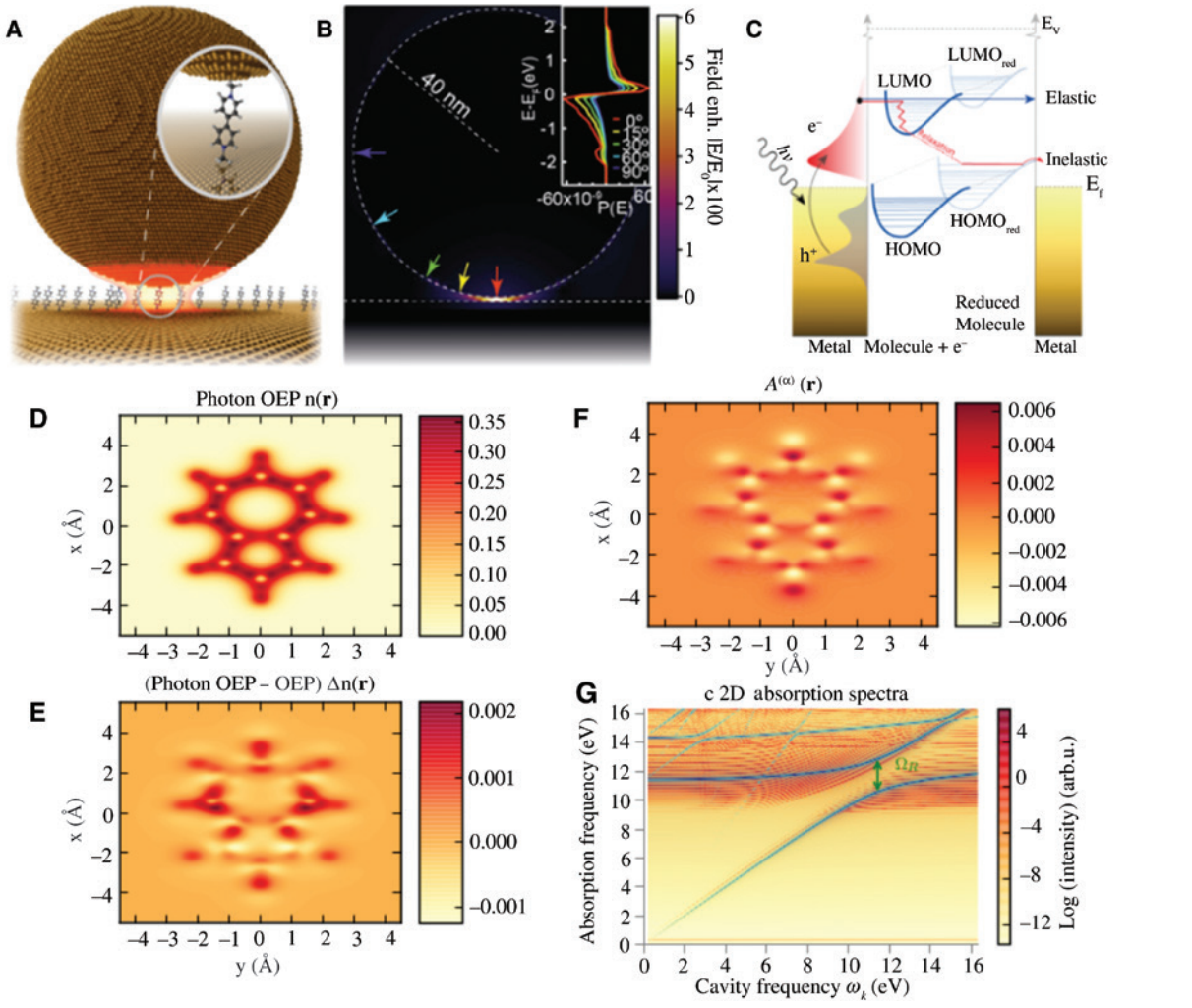

Figure 6: Novel concepts in strong light-matter coupling.
(A) Chemical molecules in plasmonic hotspots [17]. (B and C) Driving chemical reactions by hot carrier generation [17]. (D) Electron density of an azulene molecule in an optical cavity [154]. (E) Changes of the ground-state density under strong light-matter coupling calculated within the framework of QEDFT [154]. (F) New light-matter correlation functions accessible with QEDFT [154]. (G) Absorption spectra for hydrogen dimer for different cavity frequencies ω [40]. (A–C) Adapted with permission from Ref. [17]. (D–F) Adapted with permission from Ref. [154]. (G) Adapted with permission from Ref. [40] (© 2018 Springer Nature).

162], coherent excitations [163], polaritonic chemistry and multimode effects [163], static chemical systems in optical cavities and correlated spectroscopies [154], lifetimes and excited states [164], and even extended to correlated electron-nuclear motion in optical cavities [165].

4.2 General theory

In the following, we will give a brief review on the field of QEDFT and also refer the reader to the review in Ref. [40].

Although the (semi)classical approximation of the light-matter interaction is justified in the limit of strong laser pulses, in which a high number of photons occurs, this approximation breaks down in the single-photon limit [161, 163] and therefore necessitates the development of a coherent *ab initio* QED theory. As exact solutions to quantum many-body theories are usually impractical due to their unfavorable exponential scaling [155], alternative routes have to be pursued. Solutions to problems in quantum mechanics are further usually identified as finding the corresponding (ground-state) wave function of the specific problem. However, as the wave function depends on all coordinates of the system, it is a high-dimensional object that cannot even be stored on a computer hard drive for more than a few particles [155].

One alternative route is the idea of "density functionalizing" [166]. Here, a reduced object (or a set of them), i.e. a

specific observable, is chosen that does not depend on all coordinates of the system. Then, a conjugated variable is found that is usually an external control. If one now can demonstrate a so-called one-to-one correspondence (bijective mapping) between these internal and external variables, then we can completely circumvent the necessity to calculate the wave function and all solutions of the problem can be interpreted in terms of the internal variable. Thus, any observable becomes a function of this internal variable. The solution of the quantum problem is then found once the corresponding internal variable is determined.

One such method is DFT [155], where the internal variable is the electron density and the external variable is the external potential. For light-matter coupling, this specific method can be employed to any level of theory. As shown in Refs. [159, 161], in principle, such a formulation can also be formulated for the Dirac's equation to describe relativistic (anti)particles. In the nonrelativistic limit, length gauge, and dipole approximation, QEDFT is based on the one-to-one correspondence between sets of internal and external variables (for a fixed initial state Ψ_0) that can be written as follows [160]:

$$(v_{\text{ext}}(\mathbf{r}, t), j_{\text{ext}}^{(\alpha)}(t)) \overset{1:1}{\underset{\Psi_0}{\leftrightarrow}} (n(\mathbf{r}, t), q_\alpha(t)), \tag{9}$$

Here, the external variables are the electronic external potential $v_{\text{ext}}(\mathbf{r}, t)$ and the time derivative of a classical current $j_{\text{ext}}^{(\alpha)}(t)$ and allow to control the electronic and photonic subsystems, respectively. The internal variables in this limit are given by the electron density $n(\mathbf{r}, t)$ and the mode resolved displacement coordinate of photon mode α, q_α proportional to the mode-resolved displacement field $\mathbf{D}_\alpha(\mathbf{r}, t)$. Both internal variables enter in Eq. (1); further, the external Hamiltonian is defined as

$$\hat{H}_{\text{ext}}(t) = \int d\mathbf{r} v_{\text{ext}}(\mathbf{r}, t)\hat{n}(\mathbf{r}) + \sum_{\alpha=1}^{\mathcal{N}} \frac{j_{\text{ext}}^{(\alpha)}(t)}{\omega_\alpha}\hat{q}_\alpha, \tag{10}$$

where the internal variables couple to the external variables.

4.3 Kohn-Sham system

DFTs became only popular, as the one-to-one correspondence can be exploited by replacing the problem of solving an interacting many-body problem by the problem of solving a noninteracting problem. The noninteracting system is called the Kohn-Sham system [155]. In the Kohn-Sham system of QEDFT [160, 161], the interaction of Eq. (1) vanishes and the electronic degrees of freedom become decoupled from the photonic degrees of freedom. This comes with a price; however, in Eq. (10), the external potential become Kohn-Sham potentials, which have to be chosen such that they reproduce the correct many-body dynamics. Therefore, typically, we write formally

$$v_{\text{S}}(\mathbf{r}, t) = v_{\text{ext}}(\mathbf{r}, t) + v_{\text{Mxc}}(\mathbf{r}, t), \tag{11}$$

where the mean-field exchange correlation (Mxc) part now contains the effects of the electron-electron interaction as well as the electron-photon interaction. Although the mean-field part is explicitly known, for the exchange-correlation part, we have to employ approximations.

4.4 Route toward approximations

The applicability of any theory depends on its quality to predict the observable of interest. The same is true in the case of DFTs. Here, the quality of the calculation is closely intertwined with the underlying approximation for the famous exchange-correlation (xc) functional. In QEDFT, we can take advantage of existing approximation to describe the electronic structure of the system. Here, a wide range of different approximation schemes for the xc functional is available [167]. In contrast, still in its infancy, QEDFT currently lacks the rich variety of electronic DFT to choose suitable approximations. Some work has been done to close this gap, most prominently, to connect the optimized effective potential (OEP) approach to QEDFT [154, 162]. The OEP photon exchange energy can be formulated in two ways: (1) the expression of Ref. [162] depends on all occupied and unoccupied states and therefore is computationally demanding for larger systems. (2) Alternatively, the photon OEP equation and the OEP photon exchange energy can also be formulated in terms of occupied orbitals and so-called orbital shifts. These orbital shifts ($\Phi_{i\sigma,\alpha}^{(1)}$, $\Phi_{i\sigma,\alpha}^{(2)}$) are electronic wave functions and can be calculated using Sternheimer equations [154]. The photon exchange energy in terms of these orbital shifts is then given by

$$E_x^{(\alpha)}(\{\varphi_{i\sigma}\}, \{\Phi_{i\sigma,\alpha}^{(1)}\}, \{\Phi_{i\sigma,\alpha}^{(2)}\}) = \sum_{\sigma=\uparrow,\downarrow}\sum_{i=1}^{N_\sigma}\sqrt{\frac{\omega_\alpha}{8}}\langle\Phi_{i\sigma,\alpha}^{(1)}|\hat{d}_\alpha|\varphi_{i\sigma}\rangle + \frac{1}{4}\langle\Phi_{i\sigma,\alpha}^{(2)}|\hat{d}_\alpha|\varphi_{i\sigma}\rangle + c.c. \tag{12}$$

where we now have introduced so-called orbital shifts that are shifts in electronic wave functions ($\Phi_{i\sigma,\alpha}^{(1)}$, $\Phi_{i\sigma,\alpha}^{(2)}$) with spin index Φ. Whereas $\Phi_{i\sigma,\alpha}^{(1)}$ contains effects due to the one-photon processes, $\Phi_{i\sigma,\alpha}^{(2)}$ originates from the dipole self-energy term. The spin-resolved potential then follows from

$$v_{xc\sigma}(\mathbf{r}) = \frac{\delta E_{xc}}{\delta n_\sigma(\mathbf{r})}. \quad (13)$$

By formulating the OEP equation in terms of Sternheimer equations, an efficient numerical algorithm has been developed, now allowing to calculate changes in ground-state properties for coupled electron-photon systems [154], as depicted in Figure 6D, and new correlated observables [40] can be calculated as shown in Figure 6F.

4.5 Excited states

TDDFT is widely used due to its capabilities to calculate excited-state behavior of electronic systems [156]. One prominent example is the ability to calculate absorption spectra that naturally can be calculated using a linear response formalism [168]. In linear response, the system is initially in the ground state of an time-independent Hamiltonian $\hat{H}_0$. Then, a weak laser pulse that is localized in time (delta pulse) is applied to the system and its time evolution is recorded. The Fourier transform of the time-dependent dipole moment then yields the corresponding absorption spectrum [169].

When light is involved in an interaction, naturally processes occur that involve electronic excited states. In strong coupling situations, we find Rabi splitting also in spectroscopic quantities, such as the absorption spectra, as depicted in Figure 6G. Recently, a simple and numerically manageable linear response formalism has been worked out for QEDFT [164], which allows to calculate the Rabi splitting and intrinsic lifetimes from first principles.

5 Summary and perspectives/outlook

We conclude this article with a brief summary on the discussed theory methods and provide an outlook.

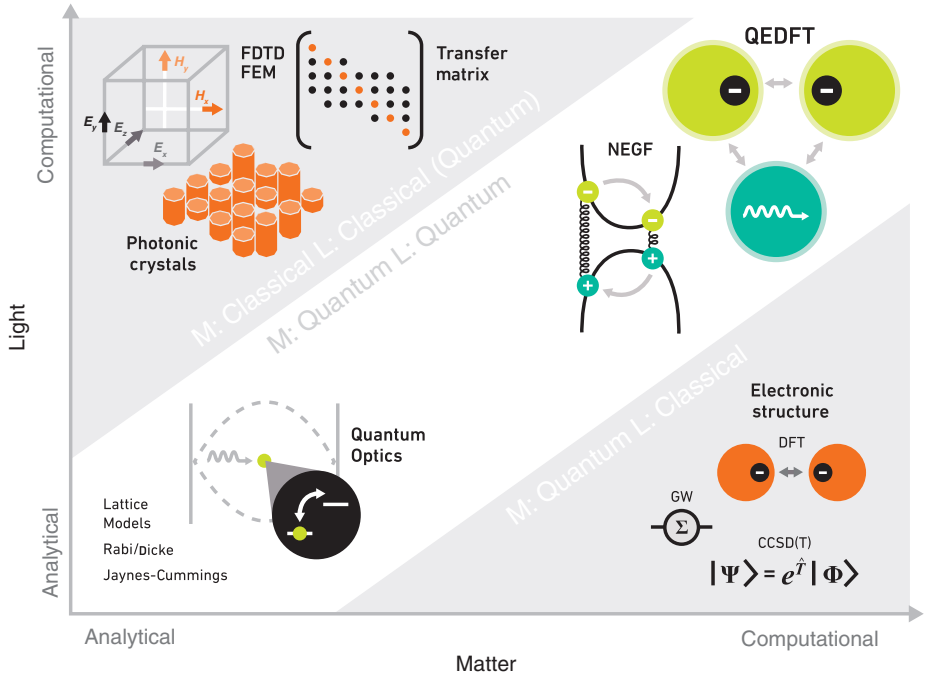

Figure 7: Theoretical methods that treat the light-matter problem can be classified by the level of theory they treat the individual subsystems and from more analytical to more computationally heavy.
More computational methods such as FDTD, FEM, photonic crystals, and the transfer matrix approach (top left) treat the matter part of the problem using classical equations of motion and the light field in great detail, mostly on the level of Maxwell's equations. In bottom right, we denote methods from the electronic structure theory such as DFT, GW, and coupled cluster [CCSD(T)] that solve the electronic Schrödinger equation and often ignore the transverse electromagnetic field effects. In the diagonal, we show methods that treat matter and light on a coherent quantized footing, such as the more analytical models heavily used in quantum optics, such as lattice models, Rabi/Dicke models, and the Jaynes-Cummings model. In top right, we depict more recent methods such as NEGF and QEDFT that treat the light-matter problem on an equally quantized level.

5.1 Summary

In Figure 7, we classify some of the current computational methods by their treatment of light and matter. In total, we classify the methods into four categories ranging from a more analytical treatment to a more computationally heavy treatment of the matter and light field, respectively. State-of-the-art methods of the electronic structure theory, such as DFT [155], many-body perturbation theory (GW) [170], or coupled cluster [171], treat the electrons quantum mechanically, and the light field on a classical level. Such methods are depicted in Figure 7 (bottom right), as they are computationally heavy on the matter part, whereas the light field is usually either not considered or taken into account only implicitly by assuming a semiclassical approximation.

Methods from nonlinear optics, the field of nanoplasmonics [172], or photonic crystals [27] are depicted in Figure 7 (top left). These methods, such as FDTD [89] and finite-element method (FEM) [173], focus on the computational aspect of the light field, and an effective treatment of the matter is employed.

In the diagonal in Figure 7, we depict methods that treat the electromagnetic field and the electronic structure on the same quantized footing. Whereas analytical solutions are often employed in quantum optics models, such as the Jaynes-Cummings model [55] (bottom left), generalized methods of the electronic structure theory such as nonequilibrium Green's function (NEGF) [174] and QEDFT [160, 161] (top right) are heavy computational methods that require massive computing power with the promise of an *ab initio* description of the combined matter-photon system.

5.2 Perspectives/outlook

Thus far, most of the works in *ab initio* many-body QED have focused on the changes to "matter observables" such as wave functions, electron energies, and chemical properties. As strong coupling by definition implies that both the matter and the photon are strongly modified, it will be of great value and interest to develop *ab initio* techniques that assess the modification of "field observables" due to light-matter coupling. Examples of interesting observables that could be tracked are the mode functions for the photons modified by matter, the new dispersion relation of the electromagnetic modes, and the amount of photons that get bound to the ground state of the correlated light-matter system [154] but also correlated light-matter correlation functions [40, 154]. What would such observables tell us? For example, if we could find how photon modes are modified by the presence of a single emitter ultra-strongly coupled to the electromagnetic field, then one could answer a very interesting fundamental question: How does a single atom modify electromagnetic modes? Can it rearrange a significant fraction of $\hbar\omega$ field energy in the vicinity of an atom? This would be analogous to how electromagnetic field modes can be altered by a dielectric inclusion. The major difference is that whereas a dielectric function description is conceptually simple for macroscopic objects, such a treatment for a single atom strongly coupled to a field is not known. Once one answers these questions, one is able to take a fundamentally new approach to quantum photonics: building waveguides and cavities with judiciously placed single emitters.

Controlling and directing reactions in single molecule-optical cavity hybrids will provide mechanistic knowledge as well as guidelines for similar quantum optical control of molecular catalytic systems. For example, chemical reactions could be performed in optical high-quality factor cavities without the need to explicitly drive the system. Conversely, these optical cavities could be used to monitor the kinetic and thermodynamic properties of chemical reactions [175], creating a new method of "quantum chemical spectroscopy".

Beyond catalysis, we envision these single molecule-optical cavity hybrids as building blocks to create novel platforms for implementing specific quantum algorithms and simulations, thereby integrating the field of quantum information with quantum chemistry [176]. Chemical systems are ultimately governed by the laws of quantum mechanics. Therefore, a quantum information perspective would provide new tools for theoretical and computational chemistry. An understanding of chemical phenomena within the framework of quantum information will shift the paradigm in theoretical chemistry by approaching problems with a different toolset.

Acknowledgments: The authors thank Professors Dirk Englund and Marin Soljacic for the discussions on experimental considerations and applications of this work and Professors Javier Aizpurua and John D. Joannopoulos for the fruitful discussions on theoretical and computational directions. Further, the authors thank group members Jennifer Coulter and Christopher Ciccarino for feedback and discussions about the review. This research used resources of the Research Computing Group at Harvard University. JF acknowledges financial support from the Deutsche Forschungsgemeinschaft (DFG) under Contract No. FL 997/1-1. N.R. was supported by Department of Energy Fellowship DE-FG02-97ER2530

(DOE CSGF). PN acknowledges funding from the Harvard John A. Paulson School of Engineering and Applied Sciences.

References

[1] Gerry C, Knight P. Introductory quantum optics. Cambridge, USA, Cambridge University Press, 2005.
[2] Lesar R. Introduction to computational materials science: fundamentals to applications, introduction to computational materials science: fundamentals to applications. New York, USA, Cambridge University Press, 2013.
[3] Iranzo DA, Nanot S, Dias EJ, et al. Probing the ultimate plasmon confinement limits with a van der Waals heterostructure. Science 2018;360:291–5.
[4] Szabo A, Ostlund N. Modern quantum chemistry: introduction to advanced electronic structure theory, dover books on chemistry. New York, USA, Dover Publications, 1989.
[5] Ebbesen TW. Hybrid Light–Matter States in a Molecular and Material Science Perspective. Acc Chem Res 2016;49:2403–12.
[6] Shalabney A, George J, Hutchison J, Pupillo G, Genet C, Ebbesen TW. Coherent coupling of molecular resonators with a microcavity mode. Nat Commun 2015;6:5981.
[7] Hutchison JA, Schwartz T, Genet C, Devaux E, Ebbesen TW. Modifying chemical landscapes by coupling to vacuum fields. Angew Chem Int Ed 2012;51:1592–6.
[8] Thomas A, George J, Shalabney A, et al. Ground-state chemical reactivity under vibrational coupling to the vacuum electromagnetic field. Angew Chem Int Ed 2016;55:11462–66.
[9] Orgiu E, George J, Hutchison JA, et al. Conductivity in organic semiconductors hybridized with the vacuum field. Nat Mater 2015;14:1123–9.
[10] Shalabney A, George J, Hiura H, et al. Enhanced raman scattering from vibro-polariton hybrid states. Angewandte Chemie 2015;127:8082–6.
[11] Slootsky M, Liu X, Menon VM, Forrest SR. Room temperature frenkel-wannier-mott hybridization of degenerate excitons in a strongly coupled microcavity. Phys Rev Lett. 2014;112:076401.
[12] Zhong X, Chervy T, Wang S, et al. Non-radiative energy transfer mediated by hybrid light-matter states. Angew Chem Int Ed 2016;55:6202–6.
[13] Zhong X, Chervy T, Zhang L, et al. Energy transfer between spatially separated entangled molecules. Angew Chem Int Ed 2017;56:9034–8.
[14] Stranius K, Hertzog M, Börjesson K. Selective manipulation of electronically excited states through strong light–matter interactions. Nat Commun 2018;9: Article ID: 2273.
[15] Kazuma E, Jung J, Ueba H, Trenary M, Kim Y. Real-space and real-time observation of a plasmon-induced chemical reaction of a single molecule. Science 2018;360:521–6.
[16] Cortes E, Xie W, Cambiasso J, et al. Plasmonic hot electron transport drives nano-localized chemistry. Nat Commun 2017;8:14880.
[17] de Nijs B, Benz F, Barrow SJ, et al. Plasmonic tunnel junctions for single-molecule redox chemistry. Nat Commun 2017;8: Article ID: 14880.
[18] Xiang B, Ribeiro RF, Dunkelberger AD, et al. Two-dimensional infrared spectroscopy of vibrational polaritons. Proc Natl Acad Sci USA 2018;115:4845–50.
[19] Chervy T, Thomas A, Akiki E, et al. Vibro-polaritonic IR emission in the strong coupling regime. ACS Photonics 2018;5:217–24.
[20] Benz F, Schmidt MK, Dreismann A, et al. Single-molecule optomechanics in "picocavities". Science 2016;354:726–29.
[21] Kasprzak J, Richard M, Kundermann S, et al. Bose–Einstein condensation of exciton polaritons. Nature 2006;443:409–14.
[22] Kongsuwan N, Demetriadou A, Chikkaraddy R, et al. Suppressed quenching and strong-coupling of purcell-enhanced single-molecule emission in plasmonic nanocavities. ACS Photonics 2018;5:186–91.
[23] Vasa P, Lienau C. Strong light–matter interaction in quantum emitter/metal hybrid nanostructures. ACS Photonics 2018; 5:2–23.
[24] Brown AM, Sundararaman R, Narang P, Schwartzberg AM, Goddard WA, Atwater HA. Experimental and Ab initio ultrafast carrier dynamics in plasmonic nanoparticles. Phys Rev Lett 2017;118:087401.
[25] Aberra Guebrou S, Symonds C, Homeyer E, et al. Coherent emission from a disordered organic semiconductor induced by strong coupling with surface plasmons. Phys Rev Lett 2012;108:066401.
[26] Santhosh K, Bitton O, Chuntonov L, Haran G. Vacuum Rabi splitting in a plasmonic cavity at the single quantum emitter limit. Nat Commun 2016;7:ncomms11823.
[27] Goban A, Hung C-L, Hood JD, et al. Superradiance for atoms trapped along a photonic crystal waveguide. Phys Rev Lett 2015;115:063601.
[28] Chikkaraddy R, de Nijs B, Benz F, et al. Single-molecule strong coupling at room temperature in plasmonic nanocavities. Nature 2016;535:127–30.
[29] Forn-Diaz P, Garcfa-Ripoll JJ, Peropadre B, et al. Ultrastrong coupling of a single artificial atom to an electromagnetic continuum in the nonperturbative regime. Nat Phys 2017;13:39–43.
[30] Liu R, Zhou Z-K, Yu Y-C, et al. Strong light-matter interactions in single open plasmonic nanocavities at the quantum optics limit. Phys Rev Lett 2017;118:237401.
[31] George J, Shalabney A, Hutchison JA, Genet C, Ebbesen TW. Liquid-phase vibrational strong coupling. J Phys Chem Lett 2015;6:1027–31.
[32] George J, Chervy T, Shalabney A, et al. Multiple rabi splittings under ultrastrong vibrational coupling. Phys Rev Lett 2016;117:153601.
[33] Coles DM, Yang Y, Wang Y, et al. Strong coupling between chlorosomes of photosynthetic bacteria and a confined optical cavity mode. Nat Commun 2014;5:5561.
[34] Coles D, Flatten LC, Sydney T, et al. A nanophotonic structure containing living photosynthetic bacteria. Small 2017;13:1701777.
[35] Wang S, Chervy T, George J, Hutchison JA, Genet C, Ebbesen TW. Quantum yield of polariton emission from hybrid light-matter states. J Phys Chem Lett 2014;5:1433–9.
[36] Todorov Y, Andrews AM, Colombelli R, et al. Ultrastrong light-matter coupling regime with polariton dots. Phys Rev Lett 2010;105:196402.
[37] Coles DM, Somaschi N, Michetti P, et al. Polariton-mediated energy transfer between organic dyes in a strongly coupled optical microcavity. Nat Mater 2014;13:712–9.

[38] Memmi H, Benson O, Sadofev S, Kalusniak S. Strong coupling between surface plasmon polaritons and molecular vibrations. Phys Rev Lett 2017;118:126802.
[39] Burek MJ, Chu Y, Liddy MSZ, et al. High quality-factor optical nanocavities in bulk single-crystal diamond. Nat Commun 2014;5: Article ID: 5718.
[40] Ruggenthaler M, Tancogne-Dejean N, Flick J, Appel H, Rubio A. From a quantum-electrodynamical light–matter description to novel spectroscopies. Nat Rev Chem 2018;2:0118.
[41] Feist J, Galego J, Garcia-Vidal FJ. Polaritonic chemistry with organic molecules. ACS Photonics 2018;5:205–16.
[42] Ribeiro RF, Martinez-Martinez LA, Du M, Campos-Gonzalez-Angulo J, Yuen-Zhou J. Polariton chemistry: controlling molecular dynamics with optical cavities. Chem Sci 2018;9: 6325–39.
[43] Forn-Dfaz P, Lamata L, Rico E, Kono J, Solano E. Ultrastrong coupling regimes of light-matter interaction. arXiv preprint arXiv:1804.09275 2018.
[44] Faisal FH. Theory of Multiphoton Processes. Berlin, Springer, 1987.
[45] Glauber RJ, Lewenstein M. Quantum optics of dielectric media. Phys Rev A 1991;43:467–91.
[46] Cohen-Tannoudji C, Dupont-Roc J, Grynberg G. Atom-photon interactions: basic processes and applications. Weinheim, Germany, Wiley-Interscience Publication. J. Wiley, 1992.
[47] Cohen-Tannoudji C, Dupont-Roc J, Grynberg G. Photons and atoms: introduction to quantum electrodynamics. Weinheim, Germany, Wiley, 1997.
[48] Craig D, Thirunamachandran T. Molecular Quantum Electrodynamics: an Introduction to Radiation-molecule Interactions, Dover Books on Chemistry Series. Orlando, FL, USA, Dover Publications, 1998.
[49] Rokaj V, Welakuh D, Ruggenthaler M, Rubio A. Light–matter interaction in the long-wavelength limit: no ground-state without dipole self-energy. J Phys B: At Mol Opt Phys 2017;51:034005.
[50] Flick J, Ruggenthaler M, Appel H, Rubio A. Atoms and molecules in cavities, from weak to strong coupling in quantum-electrodynamics (QED) chemistry. Proc Natl Acad Sci USA 2017;114:3026–34.
[51] Rabi II. On the process of space quantization. Phys Rev 1936;49:324–8.
[52] Rabi II. Space quantization in a gyrating magnetic field. Phys Rev 1937;51:652–4.
[53] Braak D. Integrability of the rabi model. Phys Rev Lett 2011;107:100401.
[54] Jaynes ET, Cummings FW. Comparison of quantum and semiclassical radiation theories with application to the beam maser. Proceedings of the IEEE 1963;51:89–109.
[55] Shore BW, Knight PL. The jaynes-cummings model. J Mod Opt 1993;40:1195–238.
[56] Haroche S, Raimond J, Press OU. Exploring the quantum: atoms, cavities, photons, oxford graduate texts. Oxford, UK, OUP Oxford, 2006.
[57] Loudon R. The quantum theory of light. Oxford, UK, OUP Oxford, 2000.
[58] Purcell EM. Spontaneous emission probabilities at radio frequencies. Phy Rev 1946;69:681.
[59] Torma P, Barnes WL. Strong coupling between surface plasmon polaritons and emitters: a review. Rep Prog Phys 2014;78:013901.
[60] Meschede D, Walther H, Muller G. One-atom maser. Phys Rev Lett 1985;54:551–4.
[61] Lidzey DG, Bradley D, Skolnick M, Virgili T, Walker S, Whittaker D. Strong exciton–photon coupling in an organic semiconductor microcavity. Nature 1998;395:53–5.
[62] Wallraff A, Schuster DI, Blais A, et al. Strong coupling of a single photon to a superconducting qubit using circuit quantum electrodynamics. Nature 2004;431:162–7.
[63] Reithmaier JP, Sek G, Loffler A, et al. Strong coupling in a single quantum dot–semiconductor microcavity system. Nature 2004;432:197–200.
[64] Peter E, Senellart P, Martrou D, et al. Exciton-photon strong-coupling regime for a single quantum dot embedded in a microcavity. Phys Rev Lett 2005;95:067401.
[65] Groblacher S, Hammerer K, Vanner MR, Aspelmeyer M. Observation of strong coupling between a micromechanical resonator and an optical cavity field. Nature 2009;460:724–7.
[66] Teufel J, Li D, Allman M, et al. Circuit cavity electromechanics in the strong-coupling regime. Nature 2011;471:204–8.
[67] Casanova J, Romero G, Lizuain I, Garcfa-Ripoll JJ, Solano E. Deep strong coupling regime of the jaynes-cummings model. Phys Rev Lett 2010;105:263603.
[68] Le Boite A, Hwang M-J, Nha H, Plenio MB. Fate of photon blockade in the deep strong-coupling regime. Phys Rev A 2016;94:033827.
[69] Niemczyk T, Deppe F, Huebl H, et al. Circuit quantum electrodynamics in the ultrastrong-coupling regime. Nat Phys 2010;6:772–6.
[70] Forn-Diaz P, Lisenfeld J, Marcos D, et al. Observation of the Bloch-Siegert shift in a Qubit-Oscillator system in the ultrastrong coupling regime. Phys Rev Lett 2010;105:237001.
[71] Yoshihara F, Fuse T, Ashhab S, Kakuyanagi K, Saito S, Semba K. Superconducting qubit–oscillator circuit beyond the ultrastrong-coupling regime. Nat Phys 2017;13:44–7.
[72] Dicke RH. Coherence in spontaneous radiation processes. Phys Rev 1954;93:99–110.
[73] Garraway BM. The Dicke model in quantum optics: Dicke model revisited. Philos Trans A Math Phys Eng Sci 2011;369:1137–55.
[74] Arias TA, Joannopoulos JD. Ab initiotheory of dislocation interactions: from close-range spontaneous annihilation to the long-range continuum limit. Phys Rev Lett 1994;73:680–3.
[75] Ralchenko Y, Jou FC, Kelleher DE, et al. NIST Atomic Spectra Database (Version 3.0), Tech. Rep. 2005.
[76] Akselrod GM, Argyropoulos C, Hoang TB, et al. Probing the mechanisms of large Purcell enhancement in plasmonic nanoantennas. Nat Photon 2014;8:835–40.
[77] Rivera N, Rosolen G, Joannopoulos JD, Kaminer I, Soljačić M. Making two-photon processes dominate one-photon processes using mid-IR phonon polaritons. Proc Natl Acad Sci USA 2017;114:13607–12.
[78] Lundeberg MB, Gao Y, Asgari R, et al. Tuning quantum nonlocal effects in graphene plasmonics. Science 2017;357:187–91.
[79] Ni G, McLeod A, Sun Z, et al. Fundamental limits to graphene plasmonics. Nature 2018;557:530–3.
[80] Caldwell JD, Glembocki OJ, Francescato Y, et al. Low-loss, extreme subdiffraction photon confinement via silicon carbide localized surface phonon polariton resonators. Nano Lett 2013;13:3690–7.
[81] Dai S, Fei Z, Ma Q, et al. Tunable phonon polaritons in atomically thin van der Waals crystals of boron nitride. Science 2014;343:1125–29.

[82] Caldwell JD, Kretinin AV, Chen Y, et al. Sub-diffractional volume-confined polaritons in the natural hyperbolic material hexagonal boron nitride. Nat Commun 2014;5:5221.
[83] Rivera N, Kaminer I, Zhen B, Joannopoulos JD, Soljačić M. Shrinking light to allow forbidden transitions on the atomic scale. Science 2016;353:263–9.
[84] Knoll L, Scheel S, Welsch D-G. QED in dispersing and absorbing media. In: Jan P., ed. Coherence and Statistics of Photons and Atoms, New York, Wiley, 2001, p. 1.
[85] Scheel S, Buhmann SY. Macroscopic quantum electrodynamics – concepts and applications. Acta Physica Slovaca 2008;58:675–809.
[86] Joannopoulos JD, Johnson SG, Winn JN, Meade RD. Photonic crystals: molding the flow of light. Princeton, NJ, USA, Princeton University Press, 2011.
[87] Taflove A, Oskooi A, Johnson SG. Advances in FDTD computational electrodynamics: photonics and nanotechnology. Boston, MA, USA, Artech House, 2013.
[88] Barnett SM, Huttner B, Loudon R. Spontaneous emission in absorbing dielectric media. Phys Rev Lett 1992;68:3698–701.
[89] Gray SK. Theory and modeling of plasmonic structures. J Phys Chem C 2013;117:1983–94.
[90] Yashiro K, Ohkawa S. Boundary element method for electromagnetic scattering from cylinders. IEEE Trans Antennas Propag 1985;33:383–9.
[91] Scholl JA, Koh AL, Dionne JA. Quantum plasmon resonances of individual metallic nanoparticles. Nature 2012;483:421–7.
[92] Savage KJ, Hawkeye MM, Esteban R, Borisov AG, Aizpurua J, Baumberg JJ. Revealing the quantum regime in tunnelling plasmonics. Nature 2012;491:574–7.
[93] Scholl JA, Garcia-Etxarri A, Koh AL, Dionne JA. Observation of quantum tunneling between two plasmonic nanoparticles. Nano Lett 2013;13:564–9.
[94] Lozan O, Sundararaman R, Ea-Kim B, et al. Increased rise time of electron temperature during adiabatic plasmon focusing. Nat Commun 2017;8:1656.
[95] Khurgin JB, Sun G. In search of the elusive lossless metal. Appl Phys Lett 2010;96:181102.
[96] Sundararaman R, Narang P, Jermyn AS, Goddard III WA, Atwater HA. Theoretical predictions for hot-carrier generation from surface plasmon decay. Nat Commun 2014;5:5788.
[97] Brown AM, Sundararaman R, Narang P, Goddard III WA, Atwater HA. Nonradiative plasmon decay and hot carrier dynamics: effects of phonons, surfaces, and geometry. ACS Nano 2016;10:957–66.
[98] Narang P, Sundararaman R, Jermyn AS, Goddard WA, Atwater HA. Cubic nonlinearity driven up-conversion in high-field plasmonic hot carrier systems. J Phys Chem C 2016;120:21056–62.
[99] Liebsch A. Electronic excitations at metal surfaces. New York, USA, Springer Science & Business Media, 2013.
[100] Raza S, Bozhevolnyi SI, Wubs M, Mortensen NA. Nonlocal optical response in metallic nanostructures. J Phys Condens Matter 2015;27:183204.
[101] Zhu W, Esteban R, Borisov AG, et al. Quantum mechanical effects in plasmonic structures with subnanometre gaps. Nat Commun 2016;7:11495.
[102] Fitzgerald JM, Narang P, Craster RV, Maier SA, Giannini V. Quantum plasmonics. Proceedings of the IEEE 2016;104:2307–22.
[103] Varas A, Garcia-Gonzalez P, Feist J, Garcia-Vidal F, Rubio A. Quantum plasmonics: from jellium models to ab initio calculations. Nanophotonics 2016;5:409.
[104] Feibelman PJ. Surface electromagnetic fields. Prog Surf Sci 1982;12:287–407.
[105] Christensen T, Yan W, Jauho A-P, Soljačić M, Mortensen NA. Quantum corrections in nanoplasmonics: shape, scale, and material. Phys Rev Lett 2017;118:157402.
[106] Zurita-Sanchez JR, Novotny L. Multipolar interband absorption in a semiconductor quantum dot I Electric quadrupole enhancement. J Opt Soc Am B 2002;19:1355.
[107] Rukhlenko ID, Handapangoda D, Premaratne M, Fedorov AV, Baranov AV, Jagadish C. Spontaneous emission of guided polaritons by quantum dot coupled to metallic nanowire: beyond the dipole approximation. Opt Express 2009;17:17570.
[108] Jain PK, Ghosh D, Baer R, Rabani E, Alivisatos AP. Near-field manipulation of spectroscopic selection rules on the nanoscale. Proc Natl Acad Sci USA 2012;109:8016–9.
[109] Kern A, Martin OJ. Strong enhancement of forbidden atomic transitions using plasmonic nanostructures. Phys Rev A 2012;85:022501.
[110] Filter R, Muhlig S, Eichelkraut T, Rockstuhl C, Lederer F. Controlling the dynamics of quantum mechanical systems sustaining dipole-forbidden transitions via optical nanoantennas. Phys Rev B 2012;86:035404.
[111] Alabastri A, Yang X, Manjavacas A, Everitt HO, Nordlander P. Extraordinary light-induced local angular momentum near metallic nanoparticles. ACS Nano 2016;10:4835–46.
[112] Machado F, Rivera N, Buljan H, Soljačić M, Kaminer I. Shaping polaritons to reshape selection rules. ACS Photonics 2018;5:3064–72.
[113] Kurman Y, Rivera N, Christensen T, et al. Inducing indirect optical transitions using graphene plasmons. Nat Photon 2018;1.
[114] Takase M, Ajiki H, Mizumoto Y, et al. Selection-rule breakdown in plasmon-induced electronic excitation of an isolated single-walled carbon nanotube. Nat Photon 2013;7:550–4.
[115] Andersen ML, Stobbe S, Sørensen AS, Lodahl P. Strongly modified plasmon–matter interaction with mesoscopic quantum emitters. Nat Phys 2011;7:215.
[116] Goppert-Mayer M. Über elementarakte mit zwei quantensprüngen. Annalen der Physik 1931;401:273–94.
[117] Breit G, Teller E. Metastability of hydrogen and helium levels. Astrophys J 1940;91:215.
[118] Hayat A, Ginzburg P, Orenstein M. Observation of two-photon emission from semiconductors. Nat Photon 2008;2:238–41.
[119] Hayat A, Nevet A, Ginzburg P, Orenstein M. Applications of two-photon processes in semiconductor photonic devices: invited review. Semicond Sci Technol 2011;26:083001.
[120] Nevet A, Berkovitch N, Hayat A, et al. Plasmonic nanoantennas for broad-band enhancement of two-photon emission from semiconductors. Nano Lett 2010;10:1848.
[121] Poddubny AN, Ginzburg P, Belov PA, Zayats AV, Kivshar YS. Tailoring and enhancing spontaneous two-photon emission using resonant plasmonic nanostructures. Phys Rev A 2012;86:033826.
[122] Aspelmeyer M, Kippenberg TJ, Marquardt F. Cavity optomechanics. Rev Mod Phys 2014;86:1391–452.

[123] Roelli P, Galland C, Piro N, Kippenberg TJ. Molecular cavity optomechanics as a theory of plasmon-enhanced Raman scattering. Nat Nanotech 2015;11:164–9.
[124] Esteban R, Borisov AG, Nordlander P, Aizpurua J. Bridging quantum and classical plasmonics with a quantum-corrected model. Nat Commun 2012;3:825.
[125] Yabana K, Sugiyama T, Shinohara Y, Otobe T, Bertsch GF. Time-dependent density functional theory for strong electromagnetic fields in crystalline solids. Phys Rev B 2012;85:045134.
[126] Feist J, Garcia-Vidal FJ. Extraordinary exciton conductance induced by strong coupling. Phys Rev Lett 2015;114:196402.
[127] Schachenmayer J, Genes C, Tignone E, Pupillo G. Cavity-enhanced transport of excitons. Phys Rev Lett 2015;114: 196403.
[128] Kumaran Y, Rivera N, Christensen T, et al. Control of semiconductor emitter frequency by increasing polariton momenta. Nat Photon 2018;12:423.
[129] Garcia-Vidal FJ, Feist J. Long-distance operator for energy transfer. Science 2017;357:1357–8.
[130] Du M, Martinez-Martinez LA, Ribeiro RF, Hu Z, Menon VM, Yuen-Zhou J. Polariton-assisted singlet fission in acene aggregates. J Phys Chem Lett 2017;9:1951–7.
[131] Saez-Blázquez R, Feist J, Fernández-Domínguez AI, García-Vidal FJ. Organic polaritons enable local vibrations to drive long-range energy transfer. Phys Rev B 2018;97: 241407.
[132] Reitz M, Mineo F, Genes C. Energy transfer and correlations in cavity-embedded donor-acceptor configurations. Sci Rep 2018;8. doi. 10.1038/s41598-018-27396-z.
[133] Hagenmuller D, Schachenmayer J, Schutz S, Genes C, Pupillo G. Cavity-enhanced transport of charge. Phys Rev Lett 2017;119:223601.
[134] Galego J, Garcia-Vidal FJ, Feist J. Suppressing photochemical reactions with quantized light fields. Nat Commun 2016;7:13841.
[135] Galego J, Garcia-Vidal FJ, Feist J. Cavity-induced modifications of molecular structure in the strong-coupling regime. Phys Rev X 2015;5:041022.
[136] Kowalewski M, Bennett K, Mukamel S. Cavity femtochemistry: manipulating nonadiabatic dynamics at avoided crossings. J Phys Chem Lett 2016;7:2050.
[137] Kowalewski M, Bennett K, Mukamel S. Non-adiabatic dynamics of molecules in optical cavities. J Chem Phys 2016;144:054309.
[138] Kowalewski M, Mukamel S. Manipulating molecules with quantum light. Proc Natl Acad Sci USA 2017;114:3278–80.
[139] Herrera F, Spano FC. Cavity-controlled chemistry in molecular ensembles. Phys Rev Lett 2016;116:238301.
[140] Martinez-Martinez LA, Ribeiro RF, Campos-Gonzalez-Angulo J, Yuen-Zhou J. Can ultrastrong coupling change ground-state chemical reactions? ACS Photonics 2018;5:167–76.
[141] Zeb MA, Kirton PG, Keeling J. Exact states and spectra of vibrationally dressed polaritons. ACS Photonics 2018;5: 249–57.
[142] Galego J, Garcia-Vidal FJ, Feist J. Many-molecule reaction triggered by a single photon in polaritonic chemistry. Phys Rev Lett 2017;119:136001.
[143] Lombardi A, Schmidt MK, Weller L, et al. Pulsed molecular optomechanics in plasmonic nanocavities: from nonlinear vibrational instabilities to bond-breaking. Phys Rev X 2018;8:011016.
[144] Sentef MA, Ruggenthaler M, Rubio A. Cavity quantum-electrodynamical polaritonically enhanced electron-phonon coupling and its influence on superconductivity. ArXiv e-prints. 2018. arXiv:1802.09437 [cond-mat.supr-con].
[145] Lindner NH, Refael G, Galitski V. Floquet topological insulator in semiconductor quantum wells. Nat Phys 2011;7:490–5.
[146] Hubener H, Sentef MA, Giovannini UD, Kemper AF, Rubio A. Creating stable Floquet–Weyl semimetals by laser-driving of 3D Dirac materials. Nat Commun 2017;8:13940.
[147] Seetharam KI, Bardyn C-E, Lindner NH, Rudner MS, Refael G. Steady state of interacting Floquet insulators. ArXiv e-prints. 2018., arXiv:1806.10620 [cond-mat.mes-hall].
[148] Flick J, Appel H, Ruggenthaler M, Rubio A. Cavity born–oppenheimer approximation for correlated electron–nuclear-photon systems. J Chem Theory Comput 2017;13:1616–25.
[149] Shin S, Metiu H. Multiple time scale quantum wavepacket propagation: electron – nuclear dynamics. J Phys Chem 1996;100:7867–72.
[150] Tully JC. Molecular dynamics with electronic transitions. J Chem Phys 1990;93:1061–71.
[151] Car R, Parrinello M. Unified approach for molecular dynamics and density-functional theory. Phys Rev Lett 1985;55:2471–74.
[152] Schafer C, Ruggenthaler M, Rubio A. Ab-initio non-relativistic quantum electrodynamics: bridging quantum chemistry and quantum optics from weak to strong coupling. ArXiv e-prints. 2018. arXiv:1804.00923 [quant-ph].
[153] Moskovits M. The case for plasmon-derived hot carrier devices. Nat Nano 2015;10:6–8.
[154] Flick J, Schafer C, Ruggenthaler M, Appel H, Rubio A. Ab initio optimized effective potentials for real molecules in optical cavities: photon contributions to the molecular ground state. ACS Photonics 2018;5:992–1005.
[155] Kohn W. Nobel Lecture: electronic structure of matter – wave functions and density functionals. Rev Mod Phys 1999;71:1253–66.
[156] Ullrich CA. Time-dependent density-functional theory: concepts and applications. Oxford, UK, OUP Oxford, 2011.
[157] Zhang P, Feist J, Rubio A, Garcia-Gonzalez P, Garcfa-Vidal FJ. Ab initionanoplasmonics: the impact of atomic structure. Phys Rev B 2014;90:161407.
[158] Vignale G, Kohn W. Current-dependent exchange-correlation potential for dynamical linear response theory. Phys Rev Lett 1996;77:2037–40.
[159] Ruggenthaler M, Mackenroth F, Bauer D. Time-dependent Kohn-Sham approach to quantum electrodynamics. Phys Rev A 2011;84:042107.
[160] Tokatly IV. Singlet-triplet conversion and the long-range proximity effect in superconductor-ferromagnet structures with generic spin dependent fields. Phys Rev Lett 2013;110:233001.
[161] Ruggenthaler M, Flick J, Pellegrini C, Appel H, Tokatly IV, Rubio A. Quantum-electrodynamical density-functional theory: bridging quantum optics and electronic-structure theory. Phys Rev A 2014;90:012508.
[162] Pellegrini C, Flick J, Tokatly IV, Appel H, Rubio A. Optimized effective potential for quantum electrodynamical time-dependent density functional theory. Phys Rev Lett 2015;115:093001.

[163] Flick J, Ruggenthaler M, Appel H, Rubio A. Kohn–Sham approach to quantum electrodynamical density-functional theory: exact time-dependent effective potentials in real space. Proc Natl Acad Sci USA 2015;112:15285–90.
[164] Flick J, Welakuh DM, Ruggenthaler M, Appel H, Rubio A. Light-matter response functions in quantum-electrodynamical density-functional theory: modifications of spectra and of the maxwell equations. arXiv preprint arXiv:1803.02519. 2018.
[165] Flick J, Narang P. Cavity correlated electron-nuclear dynamics from first principles. Phys Rev Lett 2018 (in press).
[166] Becke AD. Perspective: fifty years of density-functional theory in chemical physics. J Chem Phys 2014;140:18A301.
[167] Marques MA, Oliveira MJ, Burnus T. Libxc: a library of exchange and correlation functionals for density functional theory. Comput Phys Commun 2012;183:2272–81.
[168] Casida M, Huix-Rotllant M. Progress in time-dependent density-functional theory. Annu Rev Phys Chem 2012;63: 287–323.
[169] Marques MA, Castro A, Bertsch GF, Rubio A. Octopus: a first-principles tool for excited electron–ion dynamics Comput Phys Commun 2003;151:60–78.
[170] Onida G, Reining L, Rubio A. Electronic excitations: density-functional versus many-body Green's-function approaches. Rev Mod Phys 2002;74:601–59.
[171] Bartlett RJ, Musiał M. Coupled-cluster theory in quantum chemistry. Rev Mod Phys 2007;79:291–351.
[172] Stockman MI. Nanoplasmonics: past, present, and glimpse into future. Opt Express 2011;19:22029.
[173] Burger S, Zschiedrich L, Pomplun J, Schmidt F. Integrated optics: devices, materials, technologies XIV. In: Broquin J-E, Greiner CM, eds. Bellingham, Washington, USA, SPIE, 2010.
[174] de Melo PMMC, Marini A. Unified theory of quantized electrons, phonons, and photons out of equilibrium: a simplifiedab initioapproach based on the generalized Baym-Kadanoff ansatz. Phys Rev B 2016;93:155102.
[175] Shabani A, Roden J, Whaley KB. Continuous measurement of a non-markovian open quantum system. Phys Rev Lett 2014;112:113601.
[176] Olson J, Cao J, Romero Y, et al. Quantum information and computation for chemistry. arXiv preprint arXiv:1706.05413. 2017.